Kirchhoff–Love shells within strain gradient elasticity: weak and strong formulations and an H^3-conforming isogeometric implementation

Viacheslav Balobanov[a,1], Josef Kiendl[b], Sergei Khakalo[a], Jarkko Niiranen[a]

[a]*Aalto University, School of Engineering, Department of Civil Engineering, P.O. Box 12100, 00076 AALTO, Finland.*
[b]*NTNU, School of Engineering, Department of Marine Technology, Norway.*

Abstract

A strain gradient elasticity model for shells of arbitrary geometry is derived for the first time. The Kirchhoff–Love shell kinematics is employed in the context of a one-parameter modification of Mindlin's strain gradient elasticity theory. The weak form of the static boundary value problem of the generalized shell model is formulated within an H^3 Sobolev space setting incorporating first-, second- and third-order derivatives of the displacement variables. The strong form governing equations with a complete set of boundary conditions are derived via the principle of virtual work. A detailed description focusing on the non-standard features of the implementation of the corresponding Galerkin discretizations is provided. The numerical computations are accomplished with a conforming isogeometric method by adopting C^{p-1}-continuous NURBS basis functions of order $p \geq 3$. Convergence studies and comparisons to the corresponding three-dimensional solid element simulation verify the shell element implementation. Numerical results demonstrate the crucial capabilities of the non-standard shell model: capturing size effects and smoothening stress singularities.

Keywords: Strain gradient elasticity, Kirchhoff–Love shell, Isogeometric Analysis, Convergence, Size effects, Stress singularities

---

[1]Corresponding author, viacheslav.balobanov@aalto.fi

1. Introduction

The theories of classical continuum mechanics, relying on the principles of Cauchy's continuum from the early 19th century, have dominated the modelling of solids and structures in various fields of science and engineering during the past century [1]. During the past decades, in turn, computer methods relying on classical continuum mechanics (primarily the Finite Element Method starting from its first open-source implementations in the 1960s) have become almost omnipotent for a diverse set of complex problems of applied mechanics and engineering. Although the conventional theories of continuum mechanics have proven to be applicable for a wide range of real-life applications, they are very limited, nevertheless, in describing multi-scale phenomena which become apparent for small scale structures with dimensions comparable to material microstructure [2], architectured materials, (mechanical) metamaterials [3, 4, 5] and for the homogenization of structures of any scale with (hierarchical) substructures [6]. Moreover, it should be pointed out that the achievements of materials science and the rapid improvement of manufacturing technologies have made the production of micro- and substructures technologically and economically viable even at micro- and nano-scales (see the examples given in [5] and the references therein). According to this background, it is undeniable that the future directions of materials design and engineering applications involve materials, metamaterials and structures with manipulated or artificial micro- and substructures of different length scales.

The endeavours to extend classical continuum theories towards capturing multi-scale phenomena can be distinguished into two families of generalized theories [1]: higher-order continua such as the Cosserat continuum [7] and Mindlin's micromorphic elasticity [8]; higher-grade continua such as Mindlin's first and second strain gradient elasticity [8, 9]. In the present contribution, we concentrate on Mindlin's first strain gradient elasticity theory of Form II and, in particular, on its widely adopted single-parameter simplification having roots in [10, 11]. In general, strain gradient elasticity theories incorporating length scale parameters associated to strain gradients have shown to be capable of capturing size effects of different scales [12, 13, 14, 15, 16], smoothening nonphysical macro-scale singularities in crack tips [17, 18] or point loadings [19].

In literature, one can find a plethora of strain gradient elasticity models for bars, beams, membranes and plates, whereas regarding gradient-elastic

shell models the literature is very limited (although for higher-order (Cosserat type) shells literature is quite wide [20]). A gradient-elastic shallow shell model has been studied in [21] and governing equations of another shell model can be found in [22], whereas other studies focus on cylindrical shells: stability issues have been studied by analytical means in [23], torsional problems in [24] and wave propagation in [25]. Concerning general gradient-elastic shells of arbitrary geometry, there are no publications – neither for theoretical formulations nor for numerical methods – to our best knowledge. In fact, literature on numerical methods and analysis for gradient-elastic structural models is generally very limited, as reviewed in [26]:

"...most of existing size-dependent models focused on analytical solutions... limited to beam and plate structures subjected to certain loading and boundary conditions and geometries... Therefore, further efforts should be devoted to developing finite element models of size-dependent theories, especially the strain gradient-based models."

A few computational contributions for beams and plates already exist (see [27, 28, 15, 29, 30] utilizing Isogeometric Analysis and the references therein), while with the present work our particular aim is to liquidate the lack concerning shells: we derive the governing equations and boundary conditions as well as a variational formulation with an efficient and reliable, general-purpose numerical method for a gradient-elastic Kirchhoff–Love shell model. The variational formulation of the problem leads to an H^3 Sobolev space framework requiring C^2-continuity from the corresponding Galerkin methods. This requirement is met by adopting an isogeometric finite element approach [31] (shell approximations based on subdivision surfaces had been developed earlier in [32], in particular) with NURBS (Non-Uniform Rational B-Splines) shape functions of degree $p \geq 3$ providing C^{p-1}-continuity inside patches. The original feature of Isogeometric Analysis, performing approximate Galerkin analyses on exact NURBS-based CAD-geometries, is crucial for shape-sensitive structures such as shells. As a result, isogeometric methods for shells, particularly Kirchhoff–Love shell elements, have been a very popular research topic for almost ten years now (see [33, 34, 35, 36, 37], for instance). In the present work, the chosen method is implemented as a gradient-elastic shell user element within a commercial finite element software (Abaqus®) by utilizing the techniques developed and described in [38] for H^3-conforming plane problems of second strain gradient elasticity.

The paper is organized as follows. In section 2, we present the basics of differential geometry, classical Kirchhoff–Love shell model and general three-

dimensional theory of strain gradient elasticity. Section 3 is devoted to the derivation of the gradient-elastic Kirchhoff–Love shell model with weak and strong formulations. The corresponding numerical implementation is detailed in Section 4. Section 5 presents a set of numerical benchmark examples. Finally, in Section 6, some conclusions are drawn for future steps.

2. Preliminaries

2.1. Differential geometry of surfaces

In this subsection, we briefly recall the notations and basic definitions of differential geometry which are used in the further derivations. For more details, one is referred to [39] and [40].

We consider a curvilinear shell structure of arbitrary geometry with constant thickness h. The shell midsurface is denoted by A, with its boundary $\partial A = \Gamma$. Any point on the midsurface can be described by the radius vector $\boldsymbol{r} = \boldsymbol{r}(\theta^1, \theta^2)$ with (θ^1, θ^2) denoting the natural curvilinear surface coordinates. We also introduce coordinate θ^3 indicating the thickness direction. In what follows, we use Greek letters for indices taking values from set $\{1, 2\}$ and Latin letters for $\{1, 2, 3\}$. Einstein summation convention on repeated indices is also utilized. Herewith, a covariant basis is formed by the tangent vectors

$$\boldsymbol{a}_\alpha = \boldsymbol{r}_{,\alpha}, \tag{2.1}$$

where $(.)_{,i} = \partial(.)/\partial\theta^i$ denote the partial derivative with respect to the natural coordinate, and the unit normal vector

$$\boldsymbol{a}_3 = \frac{\boldsymbol{a}_1 \times \boldsymbol{a}_2}{|\boldsymbol{a}_1 \times \boldsymbol{a}_2|}. \tag{2.2}$$

Contravariant basis vectors $\boldsymbol{a}^j$ are defined by the following convention

$$\boldsymbol{a}_i \cdot \boldsymbol{a}^j = \delta_i^j, \tag{2.3}$$

with δ_i^j standing for the Kronecker delta.

Tensors of orders up to six, appearing in the present contribution, are defined as

$$\boldsymbol{\Phi} = \Phi^{ijk\cdots} \boldsymbol{a}_i \boldsymbol{a}_j \boldsymbol{a}_k \cdots, \tag{2.4}$$

with $\Phi^{ijk\cdots}$ being contravariant tensor components in the covariant basis $\boldsymbol{a}_i$. The components can also be represented in the contravariant or mixed bases.

In (2.4) and in what follows, we use the sequential form of writing vectors omitting the symbol of tensor multiplication $\otimes$.

Components of the covariant and contravariant metric tensors (metric coefficients) are defined, accordingly, as

$$a_{\alpha\beta} = \boldsymbol{a}_\alpha \cdot \boldsymbol{a}_\beta; \ a^{\alpha\beta} = \boldsymbol{a}^\alpha \cdot \boldsymbol{a}^\beta. \tag{2.5}$$

Co- and contravariant metric coefficients can be used for raising and lowering indices of the basis vectors as well as components of vectors and tensors in accordance with identities

$$a_{\alpha\beta}\boldsymbol{a}^\beta = \boldsymbol{a}_\alpha; \ a^{\alpha\beta}\boldsymbol{a}_\beta = \boldsymbol{a}^\alpha \tag{2.6}$$

or

$$a_{\alpha\gamma}\Phi^{\gamma\beta} = \Phi_\alpha^\beta; \ a^{\alpha\gamma}\Phi_{\gamma\beta} = \Phi_\beta^\alpha. \tag{2.7}$$

It should be mentioned that $\boldsymbol{a}_3 = \boldsymbol{a}^3$.

Along with the metric coefficients which are also called as the first fundamental form of a surface, we define the second form, namely, curvature coefficients

$$b_{\alpha\beta} = \boldsymbol{a}_{\alpha,\beta} \cdot \boldsymbol{a}_3 = -\boldsymbol{a}_\alpha \cdot \boldsymbol{a}_{3,\beta} = -\boldsymbol{a}_\beta \cdot \boldsymbol{a}_{3,\alpha}, \tag{2.8}$$

with their contravariant and mixed counterparts which can be calculated with the aid of (2.7):

$$b^{\alpha\beta} = a^{\alpha\gamma}a^{\beta\lambda}b_{\gamma\lambda}; \ b_\beta^\alpha = a^{\alpha\gamma}b_{\gamma\beta}. \tag{2.9}$$

For the purpose of taking derivatives of vectors and tensors, it is convenient to introduce the so-called covariant derivative $(.)_{|\alpha}$ which includes the derivatives of the basis vectors. With this, the partial derivative of an arbitrary vector lying in the tangent plane $\boldsymbol{v} = v^\alpha \boldsymbol{a}_\alpha = v_\alpha \boldsymbol{a}^\alpha$ is defined as

$$\boldsymbol{v}_{,i} = (v_\alpha \boldsymbol{a}^\alpha)_{,i} = v_{\alpha|i}\boldsymbol{a}^\alpha, \quad v_{\alpha|i} = v_{\alpha,i} - \Gamma_{\alpha i}^\beta v_\beta, \tag{2.10}$$

where Γ_{ji}^k denotes the Christoffel symbols of the second kind:

$$\Gamma_{ji}^k = \Gamma_{ij}^k = \boldsymbol{a}^k \cdot \boldsymbol{a}_{j,i}, \tag{2.11}$$

and with definition (2.2) $\Gamma_{\beta 3}^\alpha = -b_\beta^\alpha$, $\Gamma_{\beta\gamma}^\alpha = \boldsymbol{a}^\alpha \cdot \boldsymbol{a}_{\beta,\gamma}$. Similarly to (2.10), the covariant derivative for the contravariant vector component takes the form

$$v^\alpha{}_{|i} = v^\alpha{}_{,i} + \Gamma_{\gamma i}^\alpha v^\gamma. \tag{2.12}$$

5

For further derivations, we define the covariant derivatives of the second-order tensor components:

$$\Phi_{\alpha\beta|i} = \Phi_{\alpha\beta,i} - \Gamma^\lambda_{\alpha i}\Phi_{\lambda\beta} - \Gamma^\lambda_{\beta i}\Phi_{\alpha\lambda};$$
$$\Phi^\alpha_{\beta|i} = \Phi^\alpha_{\beta|,i} + \Gamma^\alpha_{i\lambda}\Phi^\lambda_\beta - \Gamma^\lambda_{\beta i}\Phi^\alpha_\lambda; \tag{2.13}$$
$$\Phi^{\alpha\beta}_{\ \ |i} = \Phi^{\alpha\beta}_{\ \ ,i} + \Gamma^\alpha_{i\lambda}\Phi^{\lambda\beta} + \Gamma^\beta_{i\lambda}\Phi^{\alpha\lambda}.$$

Note that by using formula (2.7) of rising and lowering indices and the fact that the covariant derivatives of metric coefficients vanish, $a_{\alpha\beta|i} = a^{\alpha\beta}_{\ \ |i} = 0$, we can calculate the derivatives of contravariant components, for instance, through the derivatives of covariant components (and vice versa):

$$\Phi^{\alpha\beta}_{\ \ |i} = a^{\alpha\gamma}a^{\beta\lambda}\Phi_{\alpha\beta|i}, \tag{2.14}$$

which is very useful in our derivations. Utilized below notation $\Phi^{\alpha\beta|\gamma}$ stands for the following:

$$\Phi^{\alpha\beta|\gamma} = \Phi^{\alpha\beta}_{\ \ |\lambda}a^{\lambda\gamma}. \tag{2.15}$$

The covariant derivative of a third-order tensor is defined as

$$\Phi^{\alpha\beta\gamma}_{\ \ \ |\lambda} = \Phi^{\alpha\beta\gamma}_{\ \ \ ,\lambda} + \Gamma^\alpha_{\rho\lambda}\Phi^{\rho\beta\gamma} + \Gamma^\beta_{\rho\lambda}\Phi^{\alpha\rho\gamma} + \Gamma^\gamma_{\rho\lambda}\Phi^{\alpha\beta\rho}, \tag{2.16}$$

and the second covariant derivative of a second-order tensor as

$$\begin{aligned}\Phi^{\alpha\beta}_{\ \ |\gamma\lambda} = \Phi^{\alpha\beta}_{\ \ ,\gamma\lambda} + \Gamma^\alpha_{\gamma\rho}\Phi^{\rho\beta}_{\ \ ,\lambda} + \Gamma^\alpha_{\gamma\rho,\lambda}\Phi^{\rho\beta} + \Gamma^\beta_{\gamma\lambda}\Phi^{\alpha\lambda}_{\ \ ,\lambda} + \Gamma^\beta_{\gamma\lambda,\lambda}\Phi^{\alpha\lambda} \\ + \Gamma^\alpha_{\lambda\rho}\Phi^{\rho\beta}_{\ \ |\gamma} + \Gamma^\beta_{\lambda\rho}\Phi^{\rho\alpha}_{\ \ |\gamma} + \Gamma^\rho_{\lambda\gamma}\Phi^{\alpha\beta}_{\ \ |\rho}.\end{aligned} \tag{2.17}$$

Note that the covariant derivative for a scalar is equal to its partial derivative:

$$u_{|\alpha} = u_{,\alpha}, \tag{2.18}$$

and the second covariant derivative is equal to

$$u_{|\alpha\beta} = u_{,\alpha\beta} - u_{,\lambda}\Gamma^\lambda_{\alpha\beta}. \tag{2.19}$$

Instead of the midsurface description of a shell structure used above, we can represent it as a three-dimensional solid body of volume $V = (-h/2, h/2) \times A$. Position vector to a body point is denoted by $\boldsymbol{x}$:

$$\boldsymbol{x} = \boldsymbol{x}(\theta^1, \theta^2, \theta^3) = \boldsymbol{r}(\theta^1, \theta^2) + \theta^3 \boldsymbol{a}_3, \quad -h/2 \leq \theta^3 \leq h/2, \tag{2.20}$$

whence it follows that the midsurface is equal to $\boldsymbol{r}(\theta^1, \theta^2) = \boldsymbol{x}(\theta^1, \theta^2, 0)$. Basis vectors are defined as

$$\boldsymbol{g}_i = \boldsymbol{x}_{,i}. \tag{2.21}$$

Similarly to (2.5), the metric coefficients of covariant basis (2.21) are equal to $g_{ij} = \boldsymbol{g}_i \cdot \boldsymbol{g}_j$. For the contravariant basis defined by an analogy with (2.3), the metric coefficients are equal to $g^{ij} = \boldsymbol{g}^i \cdot \boldsymbol{g}^j$.

A combination of (2.20) and (2.21) allows us to establish the following relation between the metric coefficients of the "solid" and "midsurface" bases (neglecting the quadratic term with respect to θ^3):

$$g_{\alpha\beta} = a_{\alpha\beta} - 2\theta^3 b_{\alpha\beta}. \tag{2.22}$$

Two vector differential operators are introduced, namely a 3D gradient $\nabla = \boldsymbol{g}^i \partial/\partial\theta^i$ and surface gradient $\nabla_S = \boldsymbol{a}^\alpha \partial/\partial\theta^\alpha$.

2.2. Shell model in classic elasticity

The deformation of a shell is described by a displacement vector $\boldsymbol{u}$ of the midsurface:

$$\boldsymbol{u} = u_\alpha \boldsymbol{a}^\alpha + u_3 \boldsymbol{a}^3. \tag{2.23}$$

Regarding the strain tensor components, the assumption that the cross sections remain normal to the midsurface allows us to neglect the transverse shear strains. The assumption of straight cross sections allows to separate the strain tensor components into two parts as

$$\varepsilon_{\alpha\beta} = \alpha_{\alpha\beta} + \theta^3 \beta_{\alpha\beta}, \tag{2.24}$$

where $\alpha_{\alpha\beta}$ and $\beta_{\alpha\beta}$ stand for the components of the first (membrane or stretching) and second (bending) strain tensors $\boldsymbol{\alpha}$ and $\boldsymbol{\beta}$, accordingly. Without going into details concerning the derivation, we introduce the kinematical assumptions in full accordance with [39]:

$$\alpha_{\alpha\beta} = \frac{1}{2}(u_{\alpha|\beta} + u_{\beta|\alpha} - 2b_{\alpha\beta}u_3), \tag{2.25}$$

$$\beta_{\alpha\beta} = -(u_{3|\alpha\beta} + b^\gamma_\alpha u_{\gamma|\beta} + b^\gamma_\beta u_{\gamma|\alpha} + b^\gamma_{\alpha|\beta} u_\gamma - b^\gamma_\alpha b_{\gamma\beta}u_3). \tag{2.26}$$

We assume that the transverse normal stress component σ^{33} is equal to zero, and the transverse shear stresses $\sigma^{\alpha3}$ do not need to be taken into account since they do not contribute into the strain energy. Therefore, here and

in what follows, we use the commonly accepted, although not fully correct, term plane stress state. Hooke's law (see (2.31) below) can be reduced to its plane-stress version:

$$\sigma^{\alpha\beta} = \widehat{C}^{\alpha\beta\gamma\rho}\varepsilon_{\gamma\rho}. \tag{2.27}$$

It should be noted that the strain component ε_{33} is not equal to zero but does not contribute into the strain energy explicitly. With the aid of the plane stress assumption, ε_{33} is expressed through the other strain components and taken into account in constitutive relation (2.27) with the plane-stress counterparts $\widehat{C}^{\alpha\beta\gamma\rho}$ of the elastic tensor components $C^{\alpha\beta\gamma\rho}$.

Analogously to strains, we introduce two stress resultants, membrane forces $\boldsymbol{n}$ and bending moments $\boldsymbol{m}$. The constitutive relations between the stress resultants and strains read as follows (based on (2.27)):

$$\boldsymbol{n} = n^{\alpha\beta}\boldsymbol{a}_\alpha\boldsymbol{a}_\beta = h\ \widehat{C}^{\alpha\beta\gamma\rho}\alpha_{\gamma\rho}\boldsymbol{a}_\alpha\boldsymbol{a}_\beta = h\ \widehat{\boldsymbol{C}} : \boldsymbol{\alpha},$$

$$\boldsymbol{m} = m^{\alpha\beta}\boldsymbol{a}_\alpha\boldsymbol{a}_\beta = \frac{h^3}{12}\ \widehat{C}^{\alpha\beta\gamma\rho}\beta_{\gamma\rho}\boldsymbol{a}_\alpha\boldsymbol{a}_\beta = \frac{h^3}{12}\ \widehat{\boldsymbol{C}} : \boldsymbol{\beta}. \tag{2.28}$$

With (2.24), (2.27), and (2.28), we can write the classical part of the strain energy variation as follows:

$$\delta W^C = \int_V \boldsymbol{\sigma} : \delta\boldsymbol{\varepsilon}\,\mathrm{d}V = \int_A (\boldsymbol{n} : \delta\boldsymbol{\alpha} + \boldsymbol{m} : \delta\boldsymbol{\beta})\,\mathrm{d}A. \tag{2.29}$$

2.3. 3D strain gradient elasticity

In the linear theory of strain gradient elasticity [8, 41], strain energy $W_{int} = W_{int}(\boldsymbol{\varepsilon}, \boldsymbol{\mu})$ is enriched by introducing the higher-order state variable $\boldsymbol{\mu} = \nabla\boldsymbol{\varepsilon}$ being the gradient of the classical strain tensor $\boldsymbol{\varepsilon} = (\nabla\boldsymbol{u} + \boldsymbol{u}\nabla)/2$ where the displacement vector $\boldsymbol{u}$ contains three translational degrees of freedom (DOFs) as within the classical elasticity theory. The variation of the strain energy in volume V, with an arbitrary variation of $\boldsymbol{u}$, takes the form

$$\delta W_{int} = \delta W^C + \delta W^\nabla = \int_V \boldsymbol{\sigma} : \delta\boldsymbol{\varepsilon}\,\mathrm{d}V + \int_V \boldsymbol{\tau} \vdots \delta\boldsymbol{\mu}\,\mathrm{d}V, \tag{2.30}$$

where the second order Cauchy-like stress tensor, the work conjugate of the strain tensor $\boldsymbol{\varepsilon}$, is denoted by $\boldsymbol{\sigma}$, whilst $\boldsymbol{\tau}$ stands for the third order double stress tensor being the work conjugate of the strain gradient tensor $\boldsymbol{\mu}$.

For the ordinary and double stress tensors, we adopt constitutive laws corresponding to the linearly elastic centrosymmetric material model (cf. [8, 17]):

$$\boldsymbol{\sigma} = \sigma^{ij}\boldsymbol{g}_i\boldsymbol{g}_j = C^{ijkl}\varepsilon_{kl}\boldsymbol{g}_i\boldsymbol{g}_j = \boldsymbol{C} : \boldsymbol{\varepsilon}, \tag{2.31}$$

standing for the generalized Hooke's law of classical elasticity and

$$\boldsymbol{\tau} = \tau^{ijk}\boldsymbol{g}_i\boldsymbol{g}_j\boldsymbol{g}_k = A^{ijklmn}\mu_{lmn}\,\boldsymbol{g}_i\boldsymbol{g}_j\boldsymbol{g}_k = \boldsymbol{A} \vdots \boldsymbol{\mu} \qquad (2.32)$$

being the higher-order analogue of the Hooke's law with respect to the double stress and strain gradient tensors. For a fully anisotropic case, the fourth-order elastic tensor $\boldsymbol{C}$ and sixth order gradient-elastic tensor $\boldsymbol{A}$ contain 21 and 171 independent moduli [42], accordingly. For practical applications, we follow Mindlin's strain gradient elasticity with separable weak non-locality [43] reducing the number of independent gradient-elastic parameters to 6. With this, the sixth-order gradient-elastic tensor $\boldsymbol{A}$ can be represented as a product of $\boldsymbol{C}$ and a second-order tensor $\boldsymbol{G}$ of length scale moduli with units of squared length, which in the index notation takes the form $A^{ijklmn} = G^{il}C^{jkmn}$.

For an isotropic case, the components of the tensor $\boldsymbol{C}$ are explicitly defined as

$$C^{ijkl} = \lambda g^{ij}g^{kl} + \mu(g^{ik}g^{jl} + g^{il}g^{jk}) \qquad (2.33)$$

bringing two independent classical elastic moduli represented by Lamé parameters μ and λ. In Cartesian coordinates, the metric coefficients coincide with the Kronecker deltas, i.e., $g^{ij} \hookrightarrow \delta^{ij}$. For isotropic materials, the second-order tensor $\boldsymbol{G}$ degenerates into a spherical tensor with the components represented by $G^{ij} = l^2 g^{ij}$ introducing a single material length scale parameter l with unit of length, which corresponds to the so-called simplified strain gradient elasticity model [11, 44]. For the components of $\boldsymbol{A}$, we can introduce the compact form

$$A^{ijklmn} = l^2 g^{il}\left[\lambda g^{jk}g^{mn} + \mu(g^{jm}g^{kn} + g^{jn}g^{km})\right] = l^2 g^{il}C^{jkmn}, \qquad (2.34)$$

which allows us to represent the double stress tensor in terms of the Cauchy-like stress tensor as

$$\boldsymbol{\tau} = l^2\nabla\boldsymbol{\sigma} = l^2\sigma^{ij|k}\boldsymbol{g}_k\boldsymbol{g}_i\boldsymbol{g}_j, \qquad (2.35)$$

which holds true only for the constant elastic moduli μ, λ. In what follows, the length scale parameter l is assumed to be constant as well. It should be mentioned that the theoretical results presented in this contribution for the one-parameter model can be extended to more general multi-parameter strain gradient elasticity theory modifications in a natural way.

9

3. Gradient-elastic Kirchhoff–Love shell model

3.1. Gradient-elastic shell model

Let us turn our attention to the additional term δW^∇ in the strain energy variation (2.30). The assumptions considered in Subsection 2.2 imply that the strain gradient tensor $\boldsymbol{\mu} = \nabla \boldsymbol{\varepsilon} = \varepsilon_{ij|k}\, \boldsymbol{g}^k \boldsymbol{g}^i \boldsymbol{g}^j$ for the Kirchhoff–Love shell model contains three sets of non-zero components $\mu_{\gamma\alpha\beta}$, $\mu_{3\alpha\beta}$ and μ_{i33}. The first one can be expressed, with the aid of (2.13) and (2.11), in the form

$$\mu_{\gamma\alpha\beta} = \varepsilon_{\alpha\beta|\gamma} = \varepsilon_{\alpha\beta,\gamma} - \Gamma^\lambda_{\alpha\gamma}\varepsilon_{\lambda\beta} - \Gamma^\lambda_{\beta\gamma}\varepsilon_{\alpha\lambda}, \tag{3.1}$$

or with (2.24) as

$$\mu_{\gamma\alpha\beta} = \alpha_{\alpha\beta|\gamma} + \theta^3 \beta_{\alpha\beta|\gamma}. \tag{3.2}$$

The second one is written as

$$\mu_{3\alpha\beta} = \varepsilon_{\alpha\beta|3} = \varepsilon_{\alpha\beta,3} + b^\lambda_\alpha \varepsilon_{\lambda\beta} + b^\lambda_\beta \varepsilon_{\alpha\lambda} = \varepsilon_{\alpha\beta,3} + \varepsilon_{\alpha\beta;3}, \tag{3.3}$$

where $\varepsilon_{\alpha\beta;3}$ denotes the difference between the covariant and partial derivatives:

$$\varepsilon_{\alpha\beta;3} = \varepsilon_{\alpha\beta|3} - \varepsilon_{\alpha\beta,3}. \tag{3.4}$$

In view of (2.24), it can be shown that $\varepsilon_{\alpha\beta,3} = \beta_{\alpha\beta}$ and $\mu_{3\alpha\beta}$ can be rewritten as:

$$\mu_{3\alpha\beta} = \beta_{\alpha\beta} + \alpha_{\alpha\beta;3} + \theta^3 \beta_{\alpha\beta;3}. \tag{3.5}$$

Likewise the classical strain component ε_{33}, the strain gradient components $\mu_{i33} = \varepsilon_{33|i}$ contribute to the strain energy implicitly.

The plane stress assumption and expression (2.35) imply the existence of 12 (9 independent) non-zero components in the double stress tensor. For them, we can write, in accordance with (2.32), a higher-order analogue of the plane-stress Hooke's law in the form

$$\tau^{i\alpha\beta} = \widehat{A}^{i\alpha\beta j\lambda\rho}\mu_{j\lambda\rho} = l^2 a^{ij}\widehat{C}^{\alpha\beta\lambda\rho}\mu_{j\lambda\rho} = l^2 \widehat{C}^{\alpha\beta\lambda\rho}\varepsilon_{\lambda\rho}|^i = l^2 \sigma^{\alpha\beta|i}. \tag{3.6}$$

In view of (2.24), (2.28), (3.5) and (3.6), let us accomplish the following

10

derivation:

$$\int_{-h/2}^{h/2} \boldsymbol{\tau} \vdots \boldsymbol{\mu} \, \mathrm{d}\theta^3 = \int_{-h/2}^{h/2} \tau^{i\alpha\beta} \mu_{i\alpha\beta} \, \mathrm{d}\theta^3$$

$$= l^2 \int_{-h/2}^{h/2} \left(\widehat{C}^{\alpha\beta\lambda\rho}(\alpha_{\lambda\rho} + \theta^3 \beta_{\lambda\rho}) \right)^{|i} \left(\alpha_{\alpha\beta} + \theta^3 \beta_{\alpha\beta} \right)_{|i} \, \mathrm{d}\theta^3$$

$$= l^2 n^{\alpha\beta|\gamma} \alpha_{\alpha\beta|\gamma} + l^2 m^{\alpha\beta|\gamma} \beta_{\alpha\beta|\gamma}$$

$$+ l^2 \int_{-h/2}^{h/2} \left((\widehat{C}^{\alpha\beta\lambda\rho} \alpha_{\lambda\rho})_{;3} + \widehat{C}^{\alpha\beta\lambda\rho} \beta_{\lambda\rho} + \theta^3 (\widehat{C}^{\alpha\beta\lambda\rho} \beta_{\lambda\rho})_{;3} \right) \left(\beta_{\alpha\beta} + \alpha_{\alpha\beta;3} + \theta^3 \beta_{\alpha\beta;3} \right) \, \mathrm{d}\theta^3$$

$$= l^2 \left(n^{\alpha\beta|\gamma} \alpha_{\alpha\beta|\gamma} + m^{\alpha\beta|\gamma} \beta_{\alpha\beta|\gamma} + m^{\alpha\beta}{}_{;3} \beta_{\alpha\beta;3} \right)$$

$$+ l^2 \left(n^{\alpha\beta}{}_{;3} + (12/h^2) m^{\alpha\beta}{}_{;3} \right) \left(\beta_{\alpha\beta} + \alpha_{\alpha\beta;3} \right),$$

$$(3.7)$$

which can be rewritten in tensor notation and inserted into the expression for the gradient-elastic part of the strain energy variation:

$$\delta W^{\nabla} = \int_V \boldsymbol{\tau} \vdots \delta\boldsymbol{\mu} \, \mathrm{d}V = \int_A \int_{-h/2}^{h/2} \boldsymbol{\tau} \vdots \delta\boldsymbol{\mu} \, \mathrm{d}\theta^3 \, \mathrm{d}A$$

$$= l^2 \int_A \left(\nabla_S \boldsymbol{n} \vdots \delta(\nabla_S \boldsymbol{\alpha}) + \nabla_S \boldsymbol{m} \vdots \delta(\nabla_S \boldsymbol{\beta}) \right) \mathrm{d}A$$

$$+ l^2 \int_A \left(\frac{12}{h^2} \boldsymbol{m} + \boldsymbol{n}_{;3} \right) : \delta \left(\boldsymbol{\beta} + \boldsymbol{\alpha}_{;3} \right) \, \mathrm{d}A$$

$$+ l^2 \int_A \left(\boldsymbol{m}_{;3} : \delta(\boldsymbol{\beta}_{;3}) \right) \, \mathrm{d}A,$$

$$(3.8)$$

where we introduce the notation $\boldsymbol{\Phi}_{;3}$ for the tensor analogue of (3.4):

$$\boldsymbol{\Phi}_{;3} = \Phi_{\alpha\beta;3} \boldsymbol{a}^{\alpha} \boldsymbol{a}^{\beta}. \qquad (3.9)$$

Remark 1. *From expression (3.8), we can see that in contrast to the classical shell theory, the strain energy is not fully decoupled into the membrane and bending parts due to the terms containing the derivative with respect to θ^3. The importance of taking into account these terms has been shown in contributions devoted to gradient-elastic Euler–Bernoulli beam models [15] and Kirchhoff plates [27, 45].*

In what follows, we use notations $\boldsymbol{t} = t^\alpha \boldsymbol{a}_\alpha$ and $\boldsymbol{\nu} = \nu^\alpha \boldsymbol{a}_\alpha$ standing, accordingly, for unit vectors tangential and normal to a boundary curve Γ of the shell midsurface and lying in a plane formed by the tangential vectors $\boldsymbol{a}_1, \boldsymbol{a}_2$ in a certain point of the boundary.

In addition to four independent boundary variables u_t, u_ν, u_3, and $u_{3,\nu}$ of the conventional Kirchhoff–Love shell model, we introduce three higher-order independent variables $u_{t,\nu}, u_{\nu,\nu}$, and $u_{3,\nu\nu}$, similar to what has been done for the gradient-elastic 2D plane (membrane) [28] and Kirchhoff plate problems [27] as well as the second strain gradient elasticity theory [9]. Here we use the following notations:

$$
\begin{aligned}
u_t &= \boldsymbol{u} \cdot \boldsymbol{t}, \quad u_\nu = \boldsymbol{u} \cdot \boldsymbol{\nu}, \\
u_{*,\nu} &= \boldsymbol{\nu} \cdot \nabla u_* = \nu^\alpha u_{*,\alpha}, \quad u_{3,\nu\nu} = \boldsymbol{\nu}\boldsymbol{\nu} : \nabla\nabla u_3 = \nu^\beta \nu^\alpha u_{3,\alpha\beta},
\end{aligned}
\tag{3.10}
$$

where the symbol $*$ takes values from the set $\{3, \nu, t\}$. Note that the non-standard boundary variables $u_{t,\nu}, u_{\nu,\nu}$ along with the standard ones u_t, u_ν associate with the membrane type boundary conditions, whereas $u_{3,\nu\nu}$ being the curvature-related boundary variable together with the rotation-related $u_{3,\nu}$ and deflection u_3 associate with the boundary conditions of bending type.

With these notations, we can construct the following expression for the variation of the virtual work performed by external forces along the variations of displacements and independent boundary variables:

$$
\begin{aligned}
\delta W_{ext} &= \int_A \boldsymbol{p} \cdot \delta \boldsymbol{u} \, \mathrm{d}A + \int_\Gamma \boldsymbol{P} \cdot \delta \boldsymbol{u} \, \mathrm{d}\Gamma + \int_\Gamma \boldsymbol{R} \cdot (\boldsymbol{\nu} \cdot \nabla \delta \boldsymbol{u}) \, \mathrm{d}\Gamma \\
&+ \int_\Gamma M(\boldsymbol{\nu} \cdot \nabla \delta u_3) \, \mathrm{d}\Gamma + \int_\Gamma \mathcal{M}(\boldsymbol{\nu}\boldsymbol{\nu} : \nabla\nabla \delta u_3) \, \mathrm{d}\Gamma.
\end{aligned}
\tag{3.11}
$$

The acting external loads are the distributed force per unit area $\boldsymbol{p} = p^1 \boldsymbol{a}_1 + p^2 \boldsymbol{a}_2 + p^3 \boldsymbol{a}_3$, traction force per unit length $\boldsymbol{P} = P^t \boldsymbol{t} + P^\nu \boldsymbol{\nu} + P^3 \boldsymbol{a}_3$, double traction force $\boldsymbol{R} = R^t \boldsymbol{t} + R^\nu \boldsymbol{\nu}$, twisting moment per unit length M, and double twisting moment $\mathcal{M}$. We assume that there are no loads applied at sharp corners.

Substituting the expressions for strain energy variations (2.29), (3.8) and variation of the work done by external forces (3.11) into the principle of virtual work

$$
\delta W = \delta(W_{ext} - W_{int}) = 0
\tag{3.12}
$$

and using constitutive expressions (2.28), we can write the weak form of the gradient-elastic Kirchhoff–Love shell problem:

Problem 1. *For $\boldsymbol{p} \in [L^2(A)]^3$, find $\boldsymbol{u} = (u_1, u_2, u_3)$, $(u_1, u_2) \in \boldsymbol{U} \subset [H^2(A)]^2$, $u_3 \in V \subset H^3(A)$ such that*

$$\mathfrak{a}(\boldsymbol{u}, \boldsymbol{v}) = \mathfrak{l}(\boldsymbol{v}) \ \forall \boldsymbol{v} = (v_1, v_2, v_3), (v_1, v_2) \in \boldsymbol{\mathcal{U}} \subset [H^2(A)]^2, v_3 \in \mathcal{V} \subset H^3(A), \tag{3.13}$$

where the bilinear form $\mathfrak{a} : (\boldsymbol{U} \times V) \times (\boldsymbol{\mathcal{U}} \times \mathcal{V}) \to \mathbb{R}$, $\mathfrak{a}(\boldsymbol{u}, \boldsymbol{v}) = \mathfrak{a}^c(\boldsymbol{u}, \boldsymbol{v}) + \mathfrak{a}^\nabla(\boldsymbol{u}, \boldsymbol{v})$, and load functional $\mathfrak{l} : \boldsymbol{\mathcal{U}} \times \mathcal{V} \to \mathbb{R}$ are defined as

$$\mathfrak{a}^c(\boldsymbol{u}, \boldsymbol{v}) = \int_A \left(h\boldsymbol{\alpha}(\boldsymbol{u}) : \widehat{\boldsymbol{C}} : \boldsymbol{\alpha}(\boldsymbol{v}) + \frac{h^3}{12}\boldsymbol{\beta}(\boldsymbol{u}) : \widehat{\boldsymbol{C}} : \boldsymbol{\beta}(\boldsymbol{v}) \right) \mathrm{d}A, \tag{3.14}$$

$$\mathfrak{a}^\nabla(\boldsymbol{u}, \boldsymbol{v}) = \int_A \left(h\nabla_S\boldsymbol{\alpha}(\boldsymbol{u}) \vdots \widehat{\boldsymbol{A}} \vdots \nabla_S\boldsymbol{\alpha}(\boldsymbol{v}) + \frac{h^3}{12}\nabla_S\boldsymbol{\beta}(\boldsymbol{u}) \vdots \widehat{\boldsymbol{A}} \vdots \nabla_S\boldsymbol{\beta}(\boldsymbol{v}) \right) \mathrm{d}A$$
$$+ l^2 \int_A \left(h\big(\boldsymbol{\beta}(\boldsymbol{u}) + \boldsymbol{\alpha}_{;3}(\boldsymbol{u})\big) : \widehat{\boldsymbol{C}} : \big(\boldsymbol{\beta}(\boldsymbol{v}) + \boldsymbol{\alpha}_{;3}(\boldsymbol{v})\big) + \frac{h^3}{12}\boldsymbol{\beta}_{;3}(\boldsymbol{u}) : \widehat{\boldsymbol{C}} : \boldsymbol{\beta}_{;3}(\boldsymbol{v}) \right) \mathrm{d}A, \tag{3.15}$$

$$\mathfrak{l}(\boldsymbol{v}) = \int_A \boldsymbol{p} \cdot \boldsymbol{v} \, \mathrm{d}A. \tag{3.16}$$

Trial function spaces $\boldsymbol{U} \subset [H^2(A)]^2$ and $V \subset H^3(A)$ should contain functions satisfying the essential boundary conditions of the problem under consideration. Accordingly, functions from test function spaces $\boldsymbol{\mathcal{U}} \subset [H^2(A)]^2$ and $\mathcal{V} \subset H^3(A)$ satisfy the corresponding homogeneous essential boundary conditions.

In the foregoing, we use notation $H^s(A)$ for a real Sobolev space of order s consisting of square integrable functions defined on A with square-integrable weak derivatives up to order s (note that $L^2 = H^0$). Components of the tensor $\widehat{\boldsymbol{A}}$ can be found in accordance with (3.6).

3.2. Strong form

In order to derive the strong form of Problem 1, we rewrite the sum of energy expressions (2.29) and (3.8) in a form similar to the one for the

classical elastic shell model:

$$\delta W_{int} = \int_A (\widetilde{\boldsymbol{n}} : \delta\boldsymbol{\alpha} + \widetilde{\boldsymbol{m}} : \delta\boldsymbol{\beta})\ \mathrm{d}A + l^2 \int_\Gamma \boldsymbol{\nu} \cdot (\nabla_S \boldsymbol{n} : \delta\boldsymbol{\alpha} + \nabla_S \boldsymbol{m} : \delta\boldsymbol{\beta})\ \mathrm{d}\Gamma,$$
(3.17)

where tensors $\widetilde{\boldsymbol{n}}$ and $\widetilde{\boldsymbol{m}}$ are defined as follows:

$$\widetilde{\boldsymbol{n}} = \left(n^{\alpha\beta} - l^2 n^{\alpha\beta}|_\gamma^\gamma + 24\frac{l^2}{h^2}m^{\gamma\beta}b_\gamma^\alpha - 2l^2(n^{\lambda\beta}b_\lambda^\gamma + n^{\gamma\lambda}b_\lambda^\beta)b_\gamma^\alpha\right)\mathbf{a}_\alpha\mathbf{a}_\beta, \quad (3.18)$$

$$\widetilde{\boldsymbol{m}} = \left((1 + 12\frac{l^2}{h^2})m^{\alpha\beta} - l^2 m^{\alpha\beta}|_\gamma^\gamma - 2l^2 n^{\gamma\beta}b_\gamma^\alpha - 2l^2(m^{\lambda\beta}b_\lambda^\gamma + m^{\gamma\lambda}b_\lambda^\beta)b_\gamma^\alpha\right)\mathbf{a}_\alpha\mathbf{a}_\beta.$$
(3.19)

Due to the symmetry of the strain tensors $\boldsymbol{\alpha}$ and $\boldsymbol{\beta}$, the first integral in (3.17) can be rewritten in the following form (with the use of (2.25) and (2.26)):

$$\int_A (\widetilde{\boldsymbol{n}} : \delta\boldsymbol{\alpha} + \widetilde{\boldsymbol{m}} : \delta\boldsymbol{\beta})\ \mathrm{d}A = \int_A \Big((\widetilde{n}^{\mathrm{sym}})^{\alpha\beta}(\delta u_{\alpha|\beta} - b_{\alpha\beta}\delta u_3)$$
$$-(\widetilde{m}^{\mathrm{sym}})^{\alpha\beta}(\delta u_{3|\alpha\beta} + 2b_\alpha^\gamma \delta u_{\gamma|\beta} + b_{\alpha|\beta}^\gamma \delta u_\gamma - b_\alpha^\gamma b_{\gamma\beta}\delta u_3)\Big)\ \mathrm{d}A,$$
(3.20)

where

$$\widetilde{\boldsymbol{n}}^{\mathrm{sym}} = \left(n^{\alpha\beta} - l^2 n^{\alpha\beta}|_\gamma^\gamma + 12\frac{l^2}{h^2}(m^{\gamma\beta}b_\gamma^\alpha + m^{\gamma\alpha}b_\gamma^\beta)\right.$$
$$\left. -l^2(n^{\lambda\beta}b_\gamma^\alpha + n^{\lambda\alpha}b_\gamma^\beta)b_\lambda^\gamma - 2l^2 n^{\gamma\lambda}b_\lambda^\beta b_\gamma^\alpha\right)\mathbf{a}_\alpha\mathbf{a}_\beta, \quad (3.21)$$

$$\widetilde{\boldsymbol{m}}^{\mathrm{sym}} = \left((1 + 12\frac{l^2}{h^2})m^{\alpha\beta} - l^2 m^{\alpha\beta}|_\gamma^\gamma - l^2(n^{\gamma\beta}b_\gamma^\alpha + n^{\gamma\alpha}b_\gamma^\beta)\right.$$
$$\left. -l^2(m^{\lambda\beta}b_\gamma^\alpha + m^{\lambda\alpha}b_\gamma^\beta)b_\lambda^\gamma - 2l^2 m^{\gamma\lambda}b_\lambda^\beta b_\gamma^\alpha\right)\mathbf{a}_\alpha\mathbf{a}_\beta. \quad (3.22)$$

By substituting (3.20) into (3.17) and accomplishing integration by parts,

<div align="center">14</div>

the variation of the internal energy takes the form

$$\delta W_{int} = \int_A \left(-(\widetilde{n}^{\mathrm{sym}})^{\alpha\beta}{}_{|\beta} + 2(\widetilde{m}^{\mathrm{sym}})^{\gamma\beta}{}_{|\beta}\, b_\gamma^\alpha + (\widetilde{m}^{\mathrm{sym}})^{\gamma\beta}\, b_{\gamma|\beta}^\alpha \right) \delta u_\alpha\, \mathrm{d}A$$

$$+ \int_A \left(-(\widetilde{n}^{\mathrm{sym}})^{\alpha\beta} b_{\alpha\beta} - (\widetilde{m}^{\mathrm{sym}})^{\alpha\beta}{}_{|\beta\alpha} + (\widetilde{m}^{\mathrm{sym}})^{\alpha\beta} b_\alpha^\gamma b_{\gamma\beta} \right) \delta u_3\, \mathrm{d}A$$

$$+ \int_\Gamma \left((\widetilde{n}^{\mathrm{sym}})^{\alpha\beta} \nu_\beta - 2(\widetilde{m}^{\mathrm{sym}})^{\gamma\beta} \nu_\beta b_\gamma^\alpha \right) \delta u_\alpha\, \mathrm{d}\Gamma$$

$$- \int_\Gamma \left((\widetilde{m}^{\mathrm{sym}})^{\alpha\beta}\, \nu_\beta \delta u_{3|\alpha} \right) \mathrm{d}\Gamma + \int_\Gamma \left((\widetilde{m}^{\mathrm{sym}})^{\alpha\beta}{}_{|\beta}\, \nu_\alpha \delta u_3 \right) \mathrm{d}\Gamma$$

$$+ l^2 \int_\Gamma \left(\nu_\alpha n^{\beta\gamma|\alpha} (\delta u_{\gamma|\beta} - b_{\beta\gamma}\delta u_3) \right) \mathrm{d}\Gamma$$

$$- l^2 \int_\Gamma \left(\nu_\alpha m^{\beta\gamma|\alpha} (\delta u_{3|\gamma\beta} + 2b_\beta^\lambda \delta u_{\lambda|\gamma} + b_{\beta|\gamma}^\lambda \delta u_\lambda - b_\beta^\lambda b_{\lambda\gamma} \delta u_3) \right) \mathrm{d}\Gamma.$$

(3.23)

With (3.23) and (3.11), the principle of virtual work (3.12) results in the strong form governing equations of the Kirchhoff–Love shell problem in the framework of the strain gradient elasticity theory:

$$(\widetilde{n}^{\mathrm{sym}})^{\alpha\beta}{}_{|\beta} - 2(\widetilde{m}^{\mathrm{sym}})^{\gamma\beta}{}_{|\beta}\, b_\gamma^\alpha - (\widetilde{m}^{\mathrm{sym}})^{\gamma\beta}\, b_{\gamma|\beta}^\alpha + p^\alpha = 0, \tag{3.24a}$$

$$(\widetilde{n}^{\mathrm{sym}})^{\alpha\beta} b_{\alpha\beta} + (\widetilde{m}^{\mathrm{sym}})^{\alpha\beta}{}_{|\beta\alpha} - (\widetilde{m}^{\mathrm{sym}})^{\alpha\beta} b_\alpha^\gamma b_{\gamma\beta} + p^3 = 0, \tag{3.24b}$$

with appropriate boundary conditions derived below.

Remark 2. *Substitutions $n^{\alpha\beta} \hookrightarrow (\widetilde{n}^{sym})^{\alpha\beta}$ and $m^{\alpha\beta} \hookrightarrow (\widetilde{m}^{sym})^{\alpha\beta}$ into (3.24) result in the governing equations of the classical Kirchhoff–Love shell model.*

Let us modify the boundary-integral terms of (3.23) separately with the use of the formulae derived in Appendix A. With the aid of (A.4), substituting $(\widetilde{m}^{\mathrm{sym}})^{\alpha\beta}\nu_\beta \hookrightarrow f^\alpha$ and $\delta u_3 \hookrightarrow u$, we have:

$$\int_\Gamma \left((\widetilde{m}^{\mathrm{sym}})^{\alpha\beta} \nu_\beta \delta u_{3|\alpha} \right) \mathrm{d}\Gamma =$$

$$- \int_\Gamma t^\gamma \left((\widetilde{m}^{\mathrm{sym}})^{\alpha\beta} \nu_\beta t_\alpha \right)_{|\gamma} \delta u_3\, \mathrm{d}\Gamma + \int_\Gamma (\widetilde{m}^{\mathrm{sym}})^{\alpha\beta} \nu_\beta \nu_\alpha \nu^\rho \delta u_{3,\rho}\, \mathrm{d}\Gamma.$$

(3.25)

Next, re-indexing in the following combination of two terms results in:

$$l^2 \int_\Gamma \left(\nu_\alpha n^{\beta\gamma|\alpha} \delta u_{\gamma|\beta} - 2\nu_\alpha m^{\beta\gamma|\alpha} b_\beta^\lambda \delta u_{\lambda|\gamma} \right) \mathrm{d}\Gamma$$

$$= l^2 \int_\Gamma \left(\nu_\gamma n^{\beta\alpha|\gamma} - 2\nu_\lambda m^{\gamma\beta|\lambda} b_\gamma^\alpha \right) \delta u_{\alpha|\beta}\, \mathrm{d}\Gamma.$$

(3.26)

15

Formula (A.2) with substitutions $(\nu_\gamma n^{\beta\alpha|\gamma} - 2\nu_\lambda m^{\gamma\beta|\lambda}b^\alpha_\gamma) \hookrightarrow \Phi^{\alpha\beta}$ and $\delta u_{\alpha|\beta} \hookrightarrow v_{\beta|\alpha}$ changes (3.26) to the following form:

$$-l^2 \int_\Gamma t^\rho \left(t_\beta(\nu_\gamma n^{\beta\alpha|\gamma} - 2\nu_\lambda m^{\gamma\beta|\lambda}b^\alpha_\gamma) \right)_{|\rho} \delta u_\alpha \, \mathrm{d}\Gamma$$
$$+ l^2 \int_\Gamma \nu_\beta(\nu_\gamma n^{\beta\alpha|\gamma} - 2\nu_\lambda m^{\gamma\beta|\lambda}b^\alpha_\gamma)\nu^\rho \delta u_{\alpha|\rho} \, \mathrm{d}\Gamma.$$

(3.27)

Finally, for the last modified term, we use (A.11) with substitutions $\nu_\alpha m^{\beta\gamma|\alpha} \hookrightarrow \Phi^{\alpha\beta}$ and $\delta u_{3|\gamma\beta} \hookrightarrow u_{,\beta\alpha}$:

$$l^2 \int_\Gamma \nu_\alpha m^{\beta\gamma|\alpha}\delta u_{3|\gamma\beta} \, \mathrm{d}\Gamma = l^2 \int_\Gamma t^\rho \left(t^\lambda(t_\beta t_\gamma \nu_\alpha m^{\beta\gamma|\alpha})_{|\lambda} \right)_{|\rho} \delta u_3 \, \mathrm{d}\Gamma$$
$$- l^2 \int_\Gamma t^\lambda \nu_\gamma(t_\beta \nu_\alpha m^{\beta\gamma|\alpha})_{|\lambda} \, \nu^\rho \delta u_{3,\rho} \, \mathrm{d}\Gamma + l^2 \int_\Gamma \nu_\beta \nu_\gamma \nu_\alpha m^{\beta\gamma|\alpha}\nu^\lambda \nu^\rho \delta u_{3,\rho\lambda} \, \mathrm{d}\Gamma$$
$$- l^2 \int_\Gamma t^\lambda(\nu_\beta t_\gamma \nu_\alpha m^{\beta\gamma|\alpha})_{|\lambda}(\nu^\rho \delta u_{3,\rho} - \delta u_3) \, \mathrm{d}\Gamma.$$

(3.28)

By the substitution of (3.25)–(3.28) into (3.23) and by utilizing the principle of virtual work (3.12), one can find the boundary conditions of the

gradient-elastic Kirchhoff–Love shell problem:

$$(\widetilde{n}^{\mathrm{sym}})^{\alpha\beta}\nu_\beta - 2(\widetilde{m}^{\mathrm{sym}})^{\gamma\beta}\nu_\beta b^\alpha_\gamma$$

$$-l^2 t^\lambda \left(t_\beta(\nu_\gamma n^{\beta\alpha|\gamma} - 2\nu_\lambda m^{\gamma\beta|\lambda}b^\alpha_\gamma)\right)_{|\lambda} - l^2\nu_\lambda m^{\beta\gamma|\lambda}b^\alpha_{\beta|\gamma} = P^\alpha \quad \text{or} \qquad (3.29\mathrm{a})$$

$$u_\alpha = \check{u}_\alpha,$$

$$(\widetilde{m}^{\mathrm{sym}})^{\alpha\beta}{}_{|\beta}\,\nu_\alpha - t^\gamma\left((\widetilde{m}^{\mathrm{sym}})^{\alpha\beta}\nu_\beta t_\alpha\right)_{|\gamma} - l^2\nu_\alpha n^{\beta\gamma|\alpha}b_{\beta\gamma}$$

$$+l^2\nu_\alpha m^{\beta\gamma|\alpha}b^\lambda_\beta b_{\lambda\gamma} + l^2 t^\rho\left(t^\lambda(t_\beta t_\gamma \nu_\alpha m^{\beta\gamma|\alpha})_{|\lambda}\right)_{|\rho}$$

$$+l^2 t^\lambda(\nu_\beta t_\gamma \nu_\alpha m^{\beta\gamma|\alpha})_{|\lambda} = P^3 \quad \text{or} \qquad (3.29\mathrm{b})$$

$$u_3 = \check{u}_3,$$

$$\nu_\beta(\nu_\gamma n^{\beta\alpha|\gamma} - 2\nu_\lambda m^{\gamma\beta|\lambda}b^\alpha_\gamma) = R^\alpha \quad \text{or}$$
$$\nu^\lambda u_{\alpha|\lambda} = \check{\varphi}_\alpha, \qquad (3.29\mathrm{c})$$

$$(\widetilde{m}^{\mathrm{sym}})^{\alpha\beta}\nu_\beta\nu_\alpha - l^2 t^\lambda \nu_\gamma(t_\beta \nu_\alpha m^{\beta\gamma|\alpha})_{|\lambda}$$
$$-l^2 t^\lambda(\nu_\beta t_\gamma \nu_\alpha m^{\beta\gamma|\alpha})_{|\lambda} = M \quad \text{or} \qquad (3.29\mathrm{d})$$

$$\nu^\rho u_{3,\rho} = \check{\omega},$$

$$l^2\nu_\beta \nu_\gamma \nu_\alpha m^{\beta\gamma|\alpha} = \mathcal{M} \quad \text{or}$$
$$\nu^\lambda \nu^\rho u_{3,\rho\lambda} = \check{\phi}, \qquad (3.29\mathrm{e})$$

where notation $(\check{.})$ stands for the prescribed values of the boundary variables.

4. Numerical implementation

The formulation of Problem 1 is written in terms of classical strain and stress resultant tensors and their derivatives. In regard to the numerical implementation, it means that we can follow the standard procedure for the classical shell element formulation (e.g. [33]) and introduce the higher-order terms as additional components. Isogeometric analysis (IGA), acting as the numerical method of the present contribution, utilizes CAD-compatible NURBS functions as the shape functions N_I, where the capital Latin index I takes integer values between 1 and N_{CP} being the total number of control points. Within IGA, as typical, we follow the isoparametric paradigm by using exactly the same NURBS functions for both the representation of the geometry and the approximations of the trial and test functions $\boldsymbol{u}^h$ and $\boldsymbol{v}^h$. In such a manner, the trial function approximation is written in a matrix

17

form as

$$\boldsymbol{u}^h = \begin{bmatrix} u_1^h \\ u_2^h \\ u_3^h \end{bmatrix} = \begin{bmatrix} N_1 & 0 & 0 & N_2 & 0 & 0 & N_3 & 0 & 0 & ... \\ 0 & N_1 & 0 & 0 & N_2 & 0 & 0 & N_3 & 0 & ... \\ 0 & 0 & N_1 & 0 & 0 & N_2 & 0 & 0 & N_3 & ... \end{bmatrix} \boldsymbol{d} = \boldsymbol{N}\boldsymbol{d},$$

(4.1)

where notation $\boldsymbol{d}$ stands for the column vector of unknown control point displacements $\boldsymbol{d} = [d_1^1\ d_2^1\ d_3^1\ d_1^2\ d_2^2\ d_3^2\ d_1^3\ d_2^3\ d_3^3\ d_1^4\ ...]^T$ with the super- and subscripts pertaining to the control point number and the displacement component u_i, respectively.

Substituting $\boldsymbol{u}^h$ and $\boldsymbol{v}^h$ in place of the exact trial and test functions $\boldsymbol{u}$ and $\boldsymbol{v}$, we rewrite Problem 1 in the standard matrix form:

$$\boldsymbol{K}\boldsymbol{d} = \boldsymbol{f},$$

(4.2)

where stiffness matrix $\boldsymbol{K}$ is defined as

$$
\begin{aligned}
\boldsymbol{K} = \int_A \Bigg(& h(\boldsymbol{T}\mathbf{L}_m\boldsymbol{N})^T \boldsymbol{D}(\boldsymbol{T}\mathbf{L}_m\boldsymbol{N}) + \frac{h^3}{12}(\boldsymbol{T}\mathbf{L}_b\boldsymbol{N})^T \boldsymbol{D}(\boldsymbol{T}\mathbf{L}_b\boldsymbol{N}) \\
& + l^2 h \left(\boldsymbol{T}_\nabla \begin{bmatrix} \mathrm{D}_1\mathbf{L}_m \\ \mathrm{D}_2\mathbf{L}_m \end{bmatrix} \boldsymbol{N} \right)^T \begin{bmatrix} \boldsymbol{D} & \boldsymbol{0} \\ \boldsymbol{0} & \boldsymbol{D} \end{bmatrix} \left(\boldsymbol{T}_\nabla \begin{bmatrix} \mathrm{D}_1\mathbf{L}_m \\ \mathrm{D}_2\mathbf{L}_m \end{bmatrix} \boldsymbol{N} \right) \\
& + l^2 \frac{h^3}{12} \left(\boldsymbol{T}_\nabla \begin{bmatrix} \mathrm{D}_1\mathbf{L}_b \\ \mathrm{D}_2\mathbf{L}_b \end{bmatrix} \boldsymbol{N} \right)^T \begin{bmatrix} \boldsymbol{D} & \boldsymbol{0} \\ \boldsymbol{0} & \boldsymbol{D} \end{bmatrix} \left(\boldsymbol{T}_\nabla \begin{bmatrix} \mathrm{D}_1\mathbf{L}_b \\ \mathrm{D}_2\mathbf{L}_b \end{bmatrix} \boldsymbol{N} \right) \\
& + l^2 h \big(\boldsymbol{T}(\mathbf{L}_b + \mathrm{D}_{\bar{3}}\mathbf{L}_m)\boldsymbol{N} \big)^T \boldsymbol{D} \big(\boldsymbol{T}(\mathbf{L}_b + \mathrm{D}_{\bar{3}}\mathbf{L}_m)\boldsymbol{N} \big) \\
& + l^2 \frac{h^3}{12} \big(\boldsymbol{T}\mathrm{D}_{\bar{3}}\mathbf{L}_b\boldsymbol{N} \big)^T \boldsymbol{D} \big(\boldsymbol{T}\mathrm{D}_{\bar{3}}\mathbf{L}_b\boldsymbol{N} \big) \Bigg) \, \mathrm{d}A,
\end{aligned}
$$

(4.3)

and the right hand side force vector $\boldsymbol{f}$ is given as

$$\boldsymbol{f} = \int_A \boldsymbol{N}^T \begin{bmatrix} p^1 \\ p^2 \\ p^3 \end{bmatrix} \, \mathrm{d}A.$$

(4.4)

In (4.3), operators $\mathbf{L}_m$ and $\mathbf{L}_b$ (see (B.1) and (B.2), accordingly) are the differential matrix operators arising in the definitions of the matrix forms for the first and second strain tensors:

$$\boldsymbol{\alpha} = \mathbf{L}_m\boldsymbol{N}\boldsymbol{d}, \quad \boldsymbol{\beta} = \mathbf{L}_b\boldsymbol{N}\boldsymbol{d},$$

(4.5)

18

where we slightly abuse the notations $\boldsymbol{\alpha}$ and $\boldsymbol{\beta}$ meaning here not tensors, as above, but column vectors containing tensor components, in accordance with Voigt notation: $\boldsymbol{\alpha} = [\alpha_{11} \ \alpha_{22} \ 2\alpha_{12}]^T$, $\boldsymbol{\beta} = [\beta_{11} \ \beta_{22} \ 2\beta_{12}]^T$. With this, the gradients of strain tensors arising in the expression for the gradient-elastic part of the strain energy (3.8) take the following matrix forms:

$$
\nabla_S \boldsymbol{\alpha} = \begin{bmatrix} \alpha_{11|1} \\ \alpha_{22|1} \\ 2\alpha_{12|1} \\ \alpha_{11|2} \\ \alpha_{22|2} \\ 2\alpha_{12|2} \end{bmatrix} = \begin{bmatrix} \mathrm{D}_1 \mathbf{L}_m \\ \\ \mathrm{D}_2 \mathbf{L}_m \end{bmatrix} \boldsymbol{N} \boldsymbol{d}, \quad \nabla_S \boldsymbol{\beta} = \begin{bmatrix} \beta_{11|1} \\ \beta_{22|1} \\ 2\beta_{12|1} \\ \beta_{11|2} \\ \beta_{22|2} \\ 2\beta_{12|2} \end{bmatrix} = \begin{bmatrix} \mathrm{D}_1 \mathbf{L}_b \\ \\ \mathrm{D}_2 \mathbf{L}_b \end{bmatrix} \boldsymbol{N} \boldsymbol{d},
$$

$$(4.6)$$

$$
\boldsymbol{\alpha}_{;3} = \begin{bmatrix} \alpha_{11;3} \\ \alpha_{22;3} \\ 2\alpha_{12;3} \end{bmatrix} = \mathrm{D}_{\bar{3}} \mathbf{L}_m \boldsymbol{N} \boldsymbol{d}, \quad \boldsymbol{\beta}_{;3} = \begin{bmatrix} \beta_{11;3} \\ \beta_{22;3} \\ 2\beta_{12;3} \end{bmatrix} = \mathrm{D}_{\bar{3}} \mathbf{L}_b \boldsymbol{N} \boldsymbol{d}. \tag{4.7}
$$

Information about the higher-order combinations of operators $\mathrm{D}_\alpha \mathbf{L}_m$, $\mathrm{D}_{\bar{3}} \mathbf{L}_m$, $\mathrm{D}_\alpha \mathbf{L}_b$, and $\mathrm{D}_{\bar{3}} \mathbf{L}_b$ can be found in Appendix B. Operator $\mathbf{L}_b$ contains the second-order derivatives itself, and in combination with D_α it engenders the third-order derivatives, which requires at least a C^2-continuous finite-element discretization. IGA with bi-cubic (and higher) NURBS shape functions naturally provide this continuity. Transformation matrices $\boldsymbol{T}$ and $\boldsymbol{T}_\nabla$ also appearing in (4.3) perform the changes of the coordinate bases. The material matrix $\boldsymbol{D}$ (see definition (C.5)) helps to establish the matrix form of the constitutive equations for stress resultants $\boldsymbol{n}$ and $\boldsymbol{m}$. More information about these matrices can be found in Appendix C.

Integration in expressions (4.3) and (4.4) can be accomplished in a standard way by applying an appropriate integration scheme including the calculation of values of the shape functions at the integration points and multiplying them by the weights with a consecutive summation. In the present contribution, we skip the detailed description of the integration process.

5. Numerical results

The lack of analytical and numerical reference solutions for the present shell problems makes the verification process more complicated. For the

purpose of testing our gradient-elastic shell element implementation, we accomplish the following steps. First, we investigate the relative increase in bending rigidity arising in micro- and nano-objects when their characteristic sizes become compatible to the length scale parameters (so-called size-effect, see Figure 5.1). Results for a bended strip modelled by the shell elements are compared to the analytical solution of the corresponding Euler–Bernoulli beam model. Second, we extend the Scordelis–Lo roof problem, a well-known benchmark example for classical shell formulations, to strain gradient elasticity. Third, a partially simply supported hyperbolic paraboloid shell affected by a concentrated load is considered and convergence of displacements and stress resultants at the point of singularity is studied. For the second and third examples, we perform a comparison with a converged reference solution obtained with 3D solid simulations for different values of the length scale parameter l.

5.1. Bending of a strip

Let us consider a bending problem of a thin strip (wide thin beam) which is clamped on one of the short edges and affected by a distributed transversal load $P_z = 1$ on the other short edge (see Figure 5.2). The problem parameters are chosen as follows: Young's modulus $E = 166000$, Poisson's ratio $\nu = 0, 0.3$, length scale parameter $l = 0, 0.05, 0.1$, length $L = 20$, width $H = 5$, thickness $h = 0.1$. A fully converged numerical solution is obtained for a model consisting of 8x32 shell elements with bi-quartic shape functions.
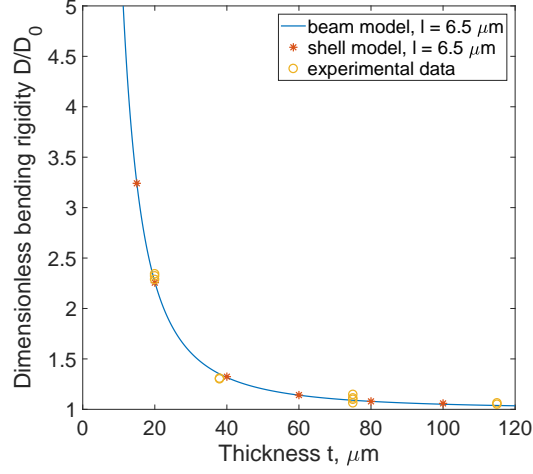
Figure 5.1: Bending of a strip (typical size effect at micro-scale). Clamped cantilever micro-beam: thickness dependence of bending rigidity D/D_0 [15, 46]
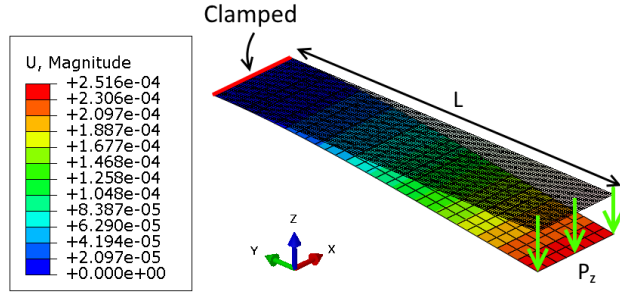
.

Figure 5.2: Bending of a strip. Problem statement and deflection for parameters $\nu = 0.3$, $l = 0.01$

.

In accordance with the Euler–Bernoulli gradient-elastic beam model, bending rigidity D_∇ normalized by the bending rigidity of the classical model D_0 for a rectangular cross section is equal to [15, 16]

$$\frac{D_\nabla}{D_0} = 1 + 12\frac{l^2}{h^2}. \tag{5.1}$$

The comparison in Table 1 between the relative bending rigidities of the (analytical) beam and (numerical) shell models reveals the agreement of the results.

	$l = 0.01$	$l = 0.05$	$l = 0.1$
D_∇/D_0, analytical beam model	1.12	4	13
D_∇/D_0, shell model ($\nu = 0$)	1.120001	4.000028	13.000100
D_∇/D_0, shell model ($\nu = 0.3$)	1.120006	4.000201	13.000787

Table 1: Bending of a strip. Comparison between the relative bending rigidities for different models and for different values of gradient-elastic parameter l

A similar size effect is observed for all the problems presented in this section. In Figure 5.1, one can also see that the shell model gives practically the same result as the Euler–Bernoulli beam model despite of the Poisson effect and both models are able to explain the experimentally observed size effect [46]. The ability of the model for capturing the size effect stems from the terms with factor l^2/h^2 in (3.18) and (3.19) (cf. [15] and [27] for beams and plates, respectively)

5.2. Scordelis–Lo roof problem

The Scordelis–Lo roof problem is one of the so-called "shell obstacle course" problems [47]. It consists of a cylindrical shell section affected by a vertical distributed area loading $p_z = -90$ (see the schema and boundary conditions in Figure 5.3a). Parameters are defined as follows: $R = 25$, $L = 50$, $\varphi = 80°$, thickness $h = 0.25$, Young's modulus $E = 4.32 \cdot 10^8$, and Poisson's ratio $\nu = 0$.

(a) Shell problem statement
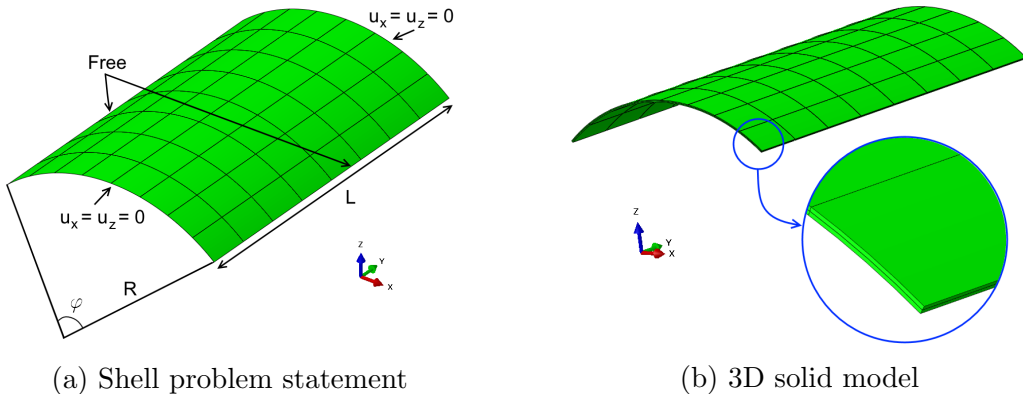
(b) 3D solid model

Figure 5.3: Scordelis–Lo roof.

Results for the maximal displacement with different values of parameter l and different basis functions orders are presented in Figure 5.4.

22
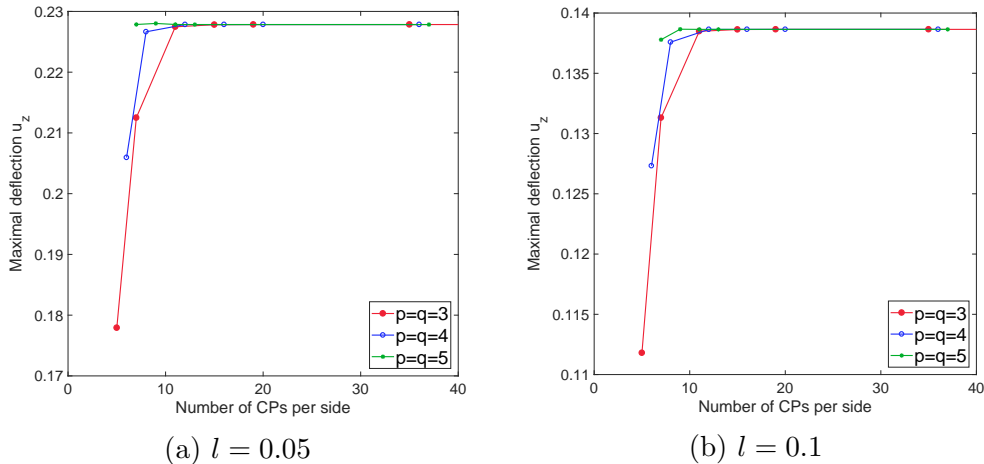
(a) $l = 0.05$ (b) $l = 0.1$

Figure 5.4: Scordelis–Lo roof. Convergence of the maximal midsurface displacement for different values of parameter l.

In order to verify the converged results, we compare them to the results of a 3D solid simulation (see the model in Figure 5.3b). The solid model consists of $128 \times 128 \times 2$ fifth-order NURBS elements. The comparison presented in Table 2 shows that the differences between the results for the shell and solid models do not exceed 0.5% for both classical and gradient-elastic versions.

	$l = 0$	$l = 0.05$	$l = 0.1$
u_z, Shell	-0.3006	-0.2278	-0.1386
u_z, Solid	-0.3015	-0.2285	-0.1391
Difference	0.30%	0.31%	0.36%

Table 2: Scordelis–Lo roof. Comparison of the midsurface maximal displacement for the shell and solid models and different values of parameter l.

5.3. Partly clamped hyperbolic paraboloid

The geometry for this problem is taken from a typical benchmarking [48] example. Let us consider a shell with a hyperbolic geometry described by $z = x^2 + y^2$, $(x, y) \in [-L/2, L/2]^2$ and depicted in Figure 5.5a. The shell body is clamped along edge $x = -L/2$ and the concentrated load P_x acts in the middle of the opposite edge (point $x = L/2, y = 0$) in the direction opposite to the x-axis. The problem parameters are given as $L = 10$, $h = 0.1$, $P_x = 1$, $E = 210000$, $\nu = 0.33$, $l = 0, 0.01$.

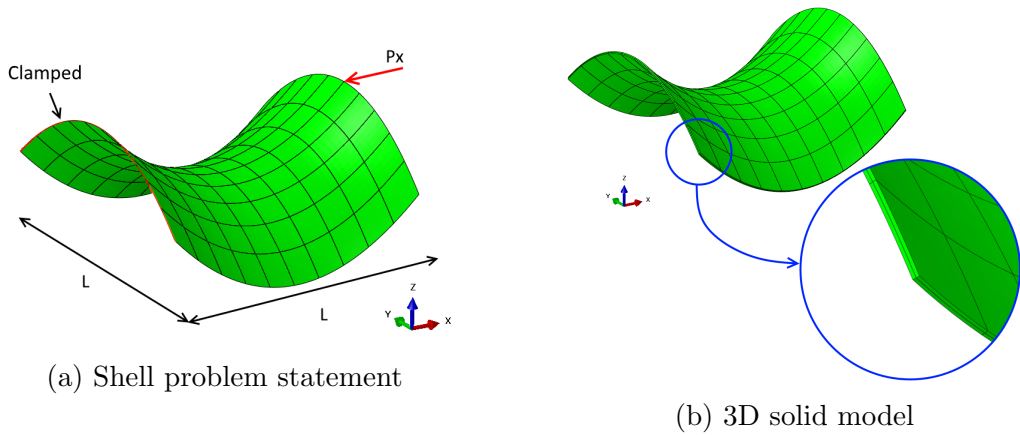(a) Shell problem statement

(b) 3D solid model

Figure 5.5: Partly clamped hyperbolic paraboloid affected by a point load.

In Figure 5.6, the convergence curves for displacements at the point of the applied load for different basis function orders are presented. The comparison with the results of 3D solid simulation (obtained for a model with $100 \times 100 \times 2$ third-order NURBS elements) shows that the differences do not exceed 5% and this holds true for both classical and gradient elasticity (see Table 3). Moreover, the simulations accomplished with the aid of the standard Finite Element Method in a commercial software Abaqus® show the same difference between shell and solid models for this problem in the framework of classical elasticity $(l = 0)$.
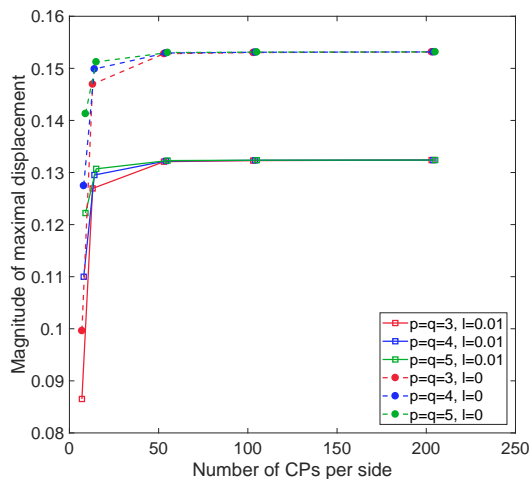
Figure 5.6: Hyperbolic paraboloid. Displacement convergence in the point of the applied load for different polynomial orders for the classical and gradient-elastic cases.

	$l = 0$	$l = 0.01$
u_z, Shell	0.1532	0.1324
u_z, Solid	0.1600	0.1393
Difference	4.25%	4.95%

Table 3: Hyperbolic paraboloid. Comparison of the midsurface maximal displacement for the shell and solid models and different values of parameter l.

Let us turn our attention to the stress resultants at the point of the applied load. At this point, direction 2 coincides with the global axis y, whereas direction 1 is perpendicular to direction 2 and belongs to the tangential plane. In Figure 5.7, we depict a convergence study for the stress resultants which are not negligibly small at the point of interest. Membrane forces n_{11} and n_{22} (Figure 5.7a,b), shear force q_1 (Figure 5.7c) and bending moment m_{22} (Figure 5.7d, in semi-logarithmic scale) increase without limit with decreasing mesh size at the point of singularity for the classical case, whilst in the framework of gradient elasticity they converge to a limited value.
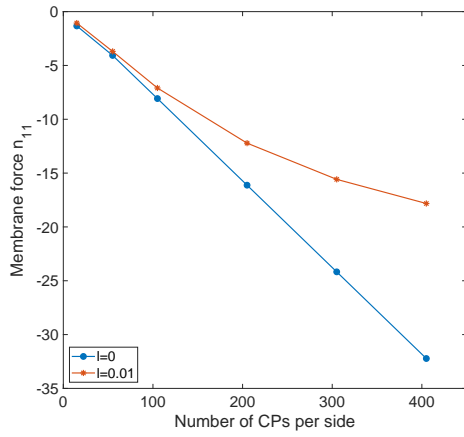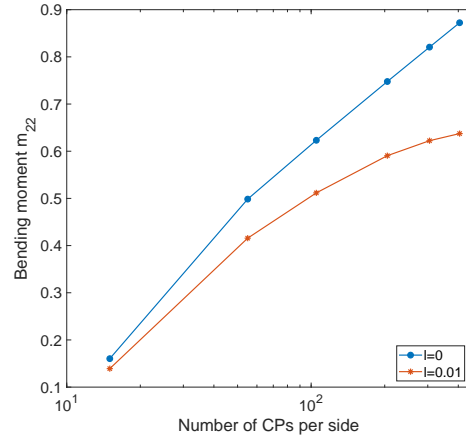
(a) Membrane force n_{11}
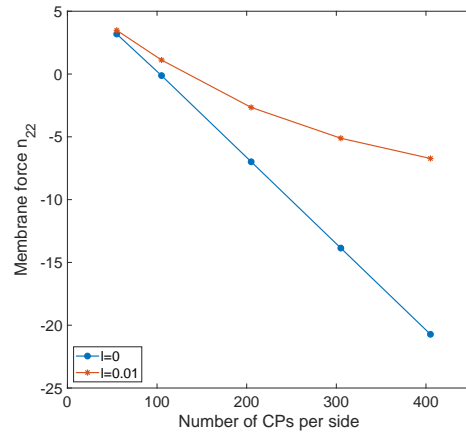
(b) Membrane force n_{22}
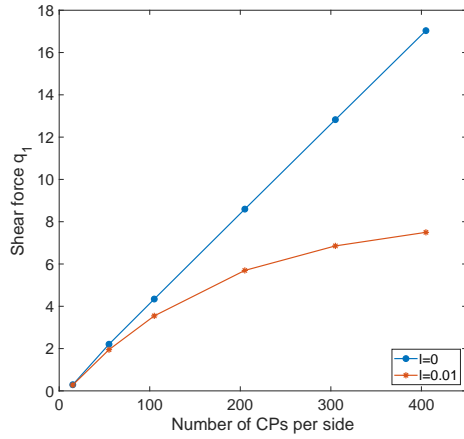
(c) Shear force q_1

(d) Bending moment m_{22}

Figure 5.7: Hyperbolic paraboloid. Non-zero stress resultants at the point of applied load.

Finally, Figure 5.8 shows the fields of membrane forces n_{11} and twisting moments m_{12} for the classical ($l = 0$) and gradient-elastic case ($l = 0.01$). One can see that the distribution of these force components is qualitatively almost identical for both cases but the maximal and minimal values are significantly different. The same observations have been made for the other forces and moments which are not presented here.
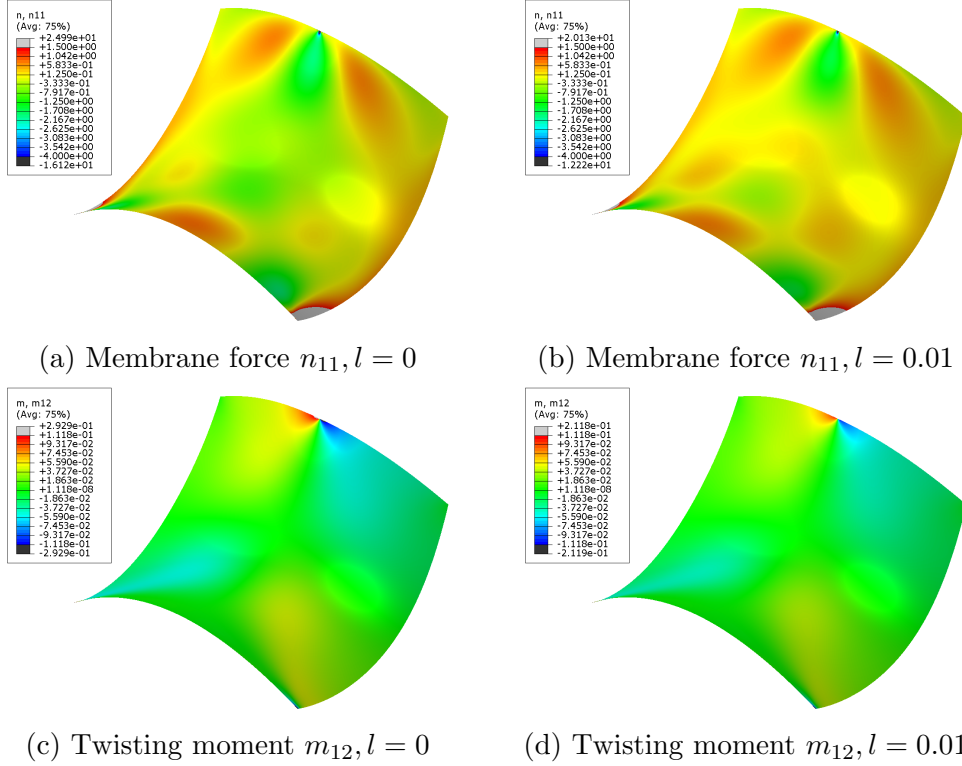
(a) Membrane force $n_{11}, l = 0$

(b) Membrane force $n_{11}, l = 0.01$

(c) Twisting moment $m_{12}, l = 0$

(d) Twisting moment $m_{12}, l = 0.01$

Figure 5.8: Hyperbolic paraboloid. Fields of stress resultants for the classical and gradient-elastic shell model with $l = 0.01$.

6. Conclusions

We have derived the governing equations, boundary conditions and variational formulation for the Kirchhoff–Love shell model in the context of a one-parameter variant of Mindlin's strain gradient elasticity theory. The corresponding numerical method based on an isogeometric C^{p-1}-continuous approach with NURBS basis functions of order $p \geq 3$ has been implemented into a commercial finite element software (Abaqus®) by adopting the so-called user element concept. The implementation has been verified and the convergence properties of the method have been confirmed by a set of benchmark problems. Regarding the shell model itself, the results demonstrate, first, that the model is able to capture the size effect related to the relative stiffening of thin micro-sized structures in bending. Second, the model is shown to avoid stress singularities at a point of a concentrated load. This example

27

demonstrates one of the properties of strain gradient elasticity: unphysical singularities presented in the classical theory of elasticity are smoothened in the strain gradient theory (see [49, 18, 50] for some examples of applications related to fracture mechanics).

For widening the applicability of the model, one of our interests is to extend the one-parameter model to a more general strain gradient model or to the cases of geometrical and material nonlinearities. Furthermore, we want to investigate the various locking mechanisms that can appear in the presented model, in particular the classical membrane locking and its gradient-elastic counterpart. The higher-order patch connections providing C^2-continuity would allow more complex shell geometries.

Acknowledgements

Appendix A. Integration by parts formulae in tensor algebra

The derivations presented here are accomplished with the aid of contribution [9].

Case 1. Notation $\boldsymbol{\Phi}$ stands for an arbitrary second-order tensor, $\boldsymbol{v} = \boldsymbol{a}^\alpha v_\alpha$ is a smooth vector function defined on a closed space curve Γ containing sharp wedges C_i:

$$\int_\Gamma \boldsymbol{\Phi} : \nabla_S \boldsymbol{v} \, \mathrm{d}\Gamma = \int_\Gamma \boldsymbol{\Phi} : (\boldsymbol{t} \, \mathrm{D}_t + \boldsymbol{\nu} \, \mathrm{D}_\nu) \boldsymbol{v} \, \mathrm{d}\Gamma$$

$$= \sum_i [\boldsymbol{t} \cdot \boldsymbol{\Phi}]_{C_i} \cdot \boldsymbol{v} - \int_\Gamma \mathrm{D}_t (\boldsymbol{t} \cdot \boldsymbol{\Phi}) \cdot \boldsymbol{v} \, \mathrm{d}\Gamma + \int_\Gamma \boldsymbol{\nu} \cdot \boldsymbol{\Phi} \cdot \mathrm{D}_\nu \boldsymbol{v} \, \mathrm{d}\Gamma,$$

$$(A.1)$$

with $D_t = \boldsymbol{t} \cdot \nabla_S$, $D_\nu = \boldsymbol{\nu} \cdot \nabla_S$ denoting the tangential and normal parts of the surface differential operator. The quantity enclosed by the brackets $[\,.\,]$ is the difference between its values on smooth pieces of the curve Γ divided by wedges C_i. Expression (A.1) can be also written in the index notations:

$$\int_\Gamma \Phi^{\alpha\beta} v_{\beta|\alpha}\, d\Gamma = \sum_i [t_\alpha \Phi^{\alpha\beta}]_{C_i} v_\beta - \int_\Gamma t^\lambda (t_\alpha \Phi^{\alpha\beta})_{|\lambda} v_\beta\, d\Gamma + \int_\Gamma \nu_\alpha \Phi^{\alpha\beta} \nu^\lambda v_{\beta|\lambda}\, d\Gamma.$$
(A.2)

Case 2. Notation $\boldsymbol{f}$ stands for an arbitrary vector field, u is a smooth scalar function defined on a closed space curve Γ:

$$\int_\Gamma \boldsymbol{f} \cdot \nabla_S u\, d\Gamma = \sum_i [\boldsymbol{f} \cdot \boldsymbol{t}\, u]_{C_i} - \int_\Gamma D_t(\boldsymbol{f} \cdot \boldsymbol{t}) u\, d\Gamma + \int_\Gamma \boldsymbol{f} \cdot \boldsymbol{\nu}\, D_\nu u\, d\Gamma. \quad \text{(A.3)}$$

Expression (A.3) in index notations is written as follows (note that $u_{|\alpha} = u_{,\alpha}$ for scalar functions):

$$\int_\Gamma f^\alpha u_{,\alpha}\, d\Gamma = \sum_i [f^\alpha t_\alpha u]_{C_i} - \int_\Gamma t^\beta (f^\alpha t_\alpha)_{|\beta}\, u\, d\Gamma + \int_\Gamma f^\alpha \nu_\alpha \nu^\beta u_{,\beta}\, d\Gamma. \quad \text{(A.4)}$$

Case 3. Combination of cases 1 and 2. Substituting $\boldsymbol{v} = \nabla_S u$ into (A.1), we can write the following:

$$\int_\Gamma \boldsymbol{\Phi} : \nabla_S \nabla_S u\, d\Gamma = \sum_i [\boldsymbol{t} \cdot \boldsymbol{\Phi} \cdot \nabla_S u]_{C_i}$$
$$- \int_\Gamma D_t(\boldsymbol{t} \cdot \boldsymbol{\Phi}) \cdot \nabla_S u\, d\Gamma + \int_\Gamma \boldsymbol{\nu} \cdot \boldsymbol{\Phi} \cdot D_\nu \nabla_S u\, d\Gamma.$$
(A.5)

Second term from the right hand side of (A.5) can be modified with the aid of (A.3) as (substituting $\boldsymbol{f} = D_t(\boldsymbol{t} \cdot \boldsymbol{\Phi})$):

$$\int_\Gamma D_t(\boldsymbol{t} \cdot \boldsymbol{\Phi}) \cdot \nabla_S u\, d\Gamma = \sum_i [D_t(\boldsymbol{t} \cdot \boldsymbol{\Phi}) \cdot \boldsymbol{t}\, u]_{C_i}$$
$$- \int_\Gamma D_t(D_t(\boldsymbol{t} \cdot \boldsymbol{\Phi}) \cdot \boldsymbol{t}) u\, d\Gamma + \int_\Gamma D_t(\boldsymbol{t} \cdot \boldsymbol{\Phi}) \cdot \boldsymbol{\nu}\, D_\nu u\, d\Gamma.$$
(A.6)

29

Next, by the use of expression

$$D_\nu \nabla_S u = \boldsymbol{\nu} \cdot \nabla_S \nabla_S u = \nabla_S(\boldsymbol{\nu} \cdot \nabla_S u) - (\nabla_S \boldsymbol{\nu}) \cdot \nabla_S u, \qquad \text{(A.7)}$$

which after the division of differential operator on the tangential and normal parts changes to

$$\boldsymbol{\nu} D_\nu^2 u + \boldsymbol{t} D_t D_\nu u - D_\nu \boldsymbol{\nu} D_\nu u - D_t \boldsymbol{\nu} D_t u = \boldsymbol{\nu} D_\nu^2 u + \boldsymbol{t} D_t D_\nu u - \boldsymbol{t} D_t u, \qquad \text{(A.8)}$$

where $D_\nu^2 = D_\nu D_\nu = (\boldsymbol{\nu} \cdot \nabla_S)(\boldsymbol{\nu} \cdot \nabla_S)$, we can write the third term from the right hand side of (A.5) as

$$\int_\Gamma \boldsymbol{\nu} \cdot \boldsymbol{\Phi} \cdot D_\nu \nabla_S u \, d\Gamma = \int_\Gamma \boldsymbol{\nu} \cdot \boldsymbol{\Phi} \cdot \boldsymbol{\nu} D_\nu^2 u \, d\Gamma + \int_\Gamma \boldsymbol{\nu} \cdot \boldsymbol{\Phi} \cdot \boldsymbol{t} D_t (D_\nu u - u) \, d\Gamma$$

$$= \int_\Gamma \boldsymbol{\nu} \cdot \boldsymbol{\Phi} \cdot \boldsymbol{\nu} D_\nu^2 u \, d\Gamma + \sum_i [\boldsymbol{\nu} \cdot \boldsymbol{\Phi} \cdot \boldsymbol{t}(D_\nu u - u)]_{C_i} - \int_\Gamma D_t(\boldsymbol{\nu} \cdot \boldsymbol{\Phi} \cdot \boldsymbol{t})(D_\nu u - u) \, d\Gamma.$$

$$\text{(A.9)}$$

Remark 3. *The derivations are done assuming that* $D_\nu \boldsymbol{\nu} = 0$.

Finally substituting (A.6) and (A.9) into (A.5), we obtain the following expression

$$\int_\Gamma \boldsymbol{\Phi} : \nabla_S \nabla_S u \, d\Gamma = \int_\Gamma D_t \left(D_t(\boldsymbol{t} \cdot \boldsymbol{\Phi}) \cdot \boldsymbol{t} \right) u \, d\Gamma - \int_\Gamma D_t(\boldsymbol{t} \cdot \boldsymbol{\Phi}) \cdot \boldsymbol{\nu} \, D_\nu u \, d\Gamma$$

$$+ \int_\Gamma \boldsymbol{\nu} \cdot \boldsymbol{\Phi} \cdot \boldsymbol{\nu} D_\nu^2 u \, d\Gamma - \int_\Gamma D_t(\boldsymbol{\nu} \cdot \boldsymbol{\Phi} \cdot \boldsymbol{t})(D_\nu u - u) \, d\Gamma,$$

$$\text{(A.10)}$$

which is written in the index form as follows:

$$\int_\Gamma \Phi^{\alpha\beta} u_{,\beta\alpha} \, d\Gamma = \int_\Gamma t^\gamma \left(t^\lambda (t_\alpha \Phi^{\alpha\beta})_{|\lambda} t_\beta \right)_{|\gamma} u \, d\Gamma$$

$$- \int_\Gamma t^\lambda (t_\alpha \Phi^{\alpha\beta})_{|\lambda} \nu_\beta \, \nu^\gamma u_{,\gamma} \, d\Gamma + \int_\Gamma \nu_\alpha \Phi^{\alpha\beta} \nu_\beta \nu^\lambda \nu^\gamma u_{,\gamma\lambda} u \, d\Gamma \qquad \text{(A.11)}$$

$$- \int_\Gamma t^\lambda (\nu_\alpha \Phi^{\alpha\beta} t_\beta)_{|\lambda} (\nu^\gamma u_{,\gamma} - u) \, d\Gamma.$$

Remark 4. *In expressions* (A.10) *and* (A.11)*, the terms related to jumps on the wedges* C_i *are omitted.*

30

Appendix B. Matrix operators $\mathbf{L}_m$ and $\mathbf{L}_b$

The matrix operators used in (4.5) have the definitions which are obtained directly from (2.25) and (2.26):

$$\mathbf{L}_m = \begin{bmatrix} D_1 & 0 & -2b_{11} \\ 0 & D_2 & -2b_{22} \\ D_2 & D_1 & -4b_{12} \end{bmatrix}, \tag{B.1}$$

$$\mathbf{L}_b = - \begin{bmatrix} 2b_1^1 D_1 + b_{1|1}^1 & 2b_1^2 D_1 + b_{1|1}^2 & D_1 D_1 - b_1^1 b_{11} - b_2^1 b_{12} \\ 2b_2^1 D_2 + b_{2|2}^1 & 2b_2^2 D_2 + b_{2|2}^2 & D_2 D_2 - b_2^1 b_{12} - b_2^2 b_{22} \\ 2b_1^1 D_2 + 2b_2^1 D_1 + 2b_{1|2}^1 & 2b_1^2 D_2 + 2b_2^2 D_1 + 2b_{1|2}^2 & 2D_1 D_2 - 2b_1^1 b_{12} - 2b_1^2 b_{22} \end{bmatrix}, \tag{B.2}$$

where notations D_1 and D_2 are used for the operators performing covariant derivation, such that $D_\alpha u_i = u_{i|\alpha}$. Operator $D_{\bar{3}}$ used below performs the following: $D_{\bar{3}} u_i = u_{i;3}$. It is worth to be mentioned that the matrix operators $\mathbf{L}_m$ and $\mathbf{L}_b$ depend on the geometric quantities, namely, curvature coefficients $b_{\alpha\beta} = b_{\alpha\beta}(\boldsymbol{r})$, $b_\alpha^\beta = b_\alpha^\beta(\boldsymbol{r})$ and their covariant derivatives which, in turn, depend on geometry point $\boldsymbol{r} = \boldsymbol{r}(\boldsymbol{N}, \boldsymbol{X})$ with $\boldsymbol{X}$ denoting the control point coordinates.

The combination of operators $D_\alpha \mathbf{L}_m$, $D_\alpha \mathbf{L}_b$, $D_{\bar{3}} \mathbf{L}_m$, $D_{\bar{3}} \mathbf{L}_b$ arising in definition of the stiffness matrix (4.3), affects their operands subsequently. However, they can be written as single higher-order matrix-operators. For instance, element [1,3] of the combination $D_1 \mathbf{L}_m$ is equal to $-2b_{11|1} - 2b_{11} D_1$.

For the Kirchhoff plate model, which is a particular case of the considered shell model, operators $\mathbf{L}_m$ and $\mathbf{L}_b$ can be simplified by setting the curvature coefficients equal to zero:

$$\mathbf{L}_m = \begin{bmatrix} D_1 & 0 & 0 \\ 0 & D_2 & 0 \\ D_2 & D_1 & 0 \end{bmatrix}, \quad \mathbf{L}_b = - \begin{bmatrix} 0 & 0 & D_1 D_1 \\ 0 & 0 & D_2 D_2 \\ 0 & 0 & 2D_1 D_2 \end{bmatrix}. \tag{B.3}$$

Structure of operators in (B.3) shows that the plate problem decouples into the bending and membrane parts, as expected.

Appendix C. Coordinate transformation matrices

It is evident that components of any tensor depend on the chosen coordinate system. So, the strain tensor in the curvilinear local base can be

expressed as $\boldsymbol{\varepsilon} = \varepsilon_{\alpha\beta}\boldsymbol{a}^\alpha\boldsymbol{a}^\beta$, whilst in the local Cartesian basis as $\boldsymbol{\varepsilon} = \bar{\varepsilon}_{\alpha\beta}\boldsymbol{e}^\alpha\boldsymbol{e}^\beta$. Components $\varepsilon_{\alpha\beta}$ and $\bar{\varepsilon}_{\alpha\beta}$ are interrelated through the formula:

$$\bar{\varepsilon}_{\lambda\rho} = \varepsilon_{\alpha\beta}(\boldsymbol{a}^\alpha \cdot \boldsymbol{e}_\lambda)(\boldsymbol{a}^\beta \cdot \boldsymbol{e}_\rho). \tag{C.1}$$

Using Voigt notation, we can write this formula in the matrix form:

$$\begin{bmatrix} \bar{\varepsilon}_{11} \\ \bar{\varepsilon}_{22} \\ 2\bar{\varepsilon}_{12} \end{bmatrix} = \boldsymbol{T} \begin{bmatrix} \varepsilon_{11} \\ \varepsilon_{22} \\ 2\varepsilon_{12} \end{bmatrix}, \tag{C.2}$$

where the transformation matrix $\boldsymbol{T}$ is defined as follows:

$$\boldsymbol{T} = \begin{bmatrix} (\boldsymbol{a}^1 \cdot \boldsymbol{e}_1)^2 & 0 & 0 \\ (\boldsymbol{a}^1 \cdot \boldsymbol{e}_2)^2 & (\boldsymbol{a}^2 \cdot \boldsymbol{e}_2)^2 & (\boldsymbol{a}^2 \cdot \boldsymbol{e}_2)(\boldsymbol{a}^1 \cdot \boldsymbol{e}_2) \\ 2(\boldsymbol{a}^1 \cdot \boldsymbol{e}_1)(\boldsymbol{a}^1 \cdot \boldsymbol{e}_2) & 0 & (\boldsymbol{a}^1 \cdot \boldsymbol{e}_1)(\boldsymbol{a}^2 \cdot \boldsymbol{e}_2) \end{bmatrix}. \tag{C.3}$$

Expression (C.3) takes into account that $\boldsymbol{e}_1 = \frac{\boldsymbol{a}_1}{|\boldsymbol{a}_1|}$ by definition and, subsequently, $\boldsymbol{a}^2 \cdot \boldsymbol{e}_1 = 0$.

Necessity of the coordinate transformation arises due to the constitutive relation:

$$\begin{bmatrix} \bar{\sigma}^{11} \\ \bar{\sigma}^{22} \\ \bar{\sigma}^{12} \end{bmatrix} = \boldsymbol{D} \begin{bmatrix} \bar{\varepsilon}_{11} \\ \bar{\varepsilon}_{22} \\ 2\bar{\varepsilon}_{12} \end{bmatrix}, \tag{C.4}$$

where $\bar{\sigma}^{\alpha\beta}$ denotes the components of Cauchy stress tensor expressed in a local Cartesian basis. The matter is that the material matrix $\boldsymbol{D}$ can be built using physical parameters only in Cartesian basis. For isotropic material it takes the form:

$$\boldsymbol{D} = \frac{E}{1 - \nu^2} \begin{bmatrix} 1 & \nu & 0 \\ \nu & 1 & 0 \\ 0 & 0 & \frac{1-\nu}{2} \end{bmatrix}. \tag{C.5}$$

Note that formula (C.2) can be applied for transformation of the components of tensors $\boldsymbol{\alpha}$ and $\boldsymbol{\beta}$ without any modifications of matrix $\boldsymbol{T}$. By analogy with (C.4), we can write the matrix forms of constitutive law (2.28) for the stress resultants:

$$\begin{bmatrix} \bar{n}^{11} \\ \bar{n}^{22} \\ \bar{n}^{12} \end{bmatrix} = h \, \boldsymbol{D} \begin{bmatrix} \bar{\alpha}_{11} \\ \bar{\alpha}_{22} \\ 2\bar{\alpha}_{12} \end{bmatrix}, \qquad \begin{bmatrix} \bar{m}^{11} \\ \bar{m}^{22} \\ \bar{m}^{12} \end{bmatrix} = \frac{h^3}{12} \, \boldsymbol{D} \begin{bmatrix} \bar{\beta}_{11} \\ \bar{\beta}_{22} \\ 2\bar{\beta}_{12} \end{bmatrix}. \tag{C.6}$$

Regarding the gradient-elastic analogues of expression (C.6), the following can be established. Tensors $\boldsymbol{\tau}$ and $\boldsymbol{\mu}$ and, accordingly, their resultants and parts $\nabla \boldsymbol{n}$, $\nabla \boldsymbol{m}$ and $\nabla \boldsymbol{\alpha}$, $\nabla \boldsymbol{\beta}$, include 9 non-zero independent components each. With the aid of Voigt notation, we can write the following constitutive laws in the matrix form ($i = \{1, 2, 3\}$):

$$
\begin{bmatrix} \bar{n}^{11|i} \\ \bar{n}^{22|i} \\ \bar{n}^{12|i} \end{bmatrix} = h \, \boldsymbol{D} \begin{bmatrix} \bar{\alpha}_{11|i} \\ \bar{\alpha}_{22|i} \\ 2\bar{\alpha}_{12|i} \end{bmatrix}, \qquad \begin{bmatrix} \bar{m}^{11|i} \\ \bar{m}^{22|i} \\ \bar{m}^{12|i} \end{bmatrix} = \frac{h^3}{12} \, \boldsymbol{D} \begin{bmatrix} \bar{\beta}_{11|i} \\ \bar{\beta}_{22|i} \\ 2\bar{\beta}_{12|i} \end{bmatrix}. \tag{C.7}
$$

Similarly to (C.1), the transformation rule for the third-order tensor is written as

$$
\bar{\mu}_{\lambda\rho\delta} = \mu_{\alpha\beta\gamma}(\boldsymbol{a}^\alpha \cdot \boldsymbol{e}_\lambda)(\boldsymbol{a}^\beta \cdot \boldsymbol{e}_\rho)(\boldsymbol{a}^\gamma \cdot \boldsymbol{e}_\delta), \tag{C.8}
$$

and in the matrix form as

$$
\begin{bmatrix} \bar{\mu}_{111} \\ \bar{\mu}_{122} \\ 2\bar{\mu}_{112} \\ \bar{\mu}_{211} \\ \bar{\mu}_{222} \\ 2\bar{\mu}_{212} \end{bmatrix} = \boldsymbol{T}_\nabla \begin{bmatrix} \mu_{111} \\ \mu_{122} \\ 2\mu_{112} \\ \mu_{211} \\ \mu_{222} \\ 2\mu_{212} \end{bmatrix}, \tag{C.9}
$$

where the higher-order transformation matrix $\boldsymbol{T}_\nabla$ is defined as

$$
\boldsymbol{T}_\nabla = \begin{bmatrix} T_{111111} & 0 & 0 & 0 & 0 & 0 \\ T_{111111} & T_{112222} & T_{112122} & 0 & 0 & 0 \\ T_{111111} & 0 & T_{111122} & 0 & 0 & 0 \\ T_{211111} & 0 & 0 & T_{221111} & 0 & 0 \\ T_{212121} & T_{212222} & T_{212122} & T_{222121} & T_{222222} & T_{222122} \\ T_{211121} & 0 & T_{211122} & T_{221121} & 0 & T_{221122} \end{bmatrix}, \tag{C.10}
$$

with $T_{\alpha\lambda\beta\rho\gamma\delta} = (\boldsymbol{a}^\alpha \cdot \boldsymbol{e}_\lambda)(\boldsymbol{a}^\beta \cdot \boldsymbol{e}_\rho)(\boldsymbol{a}^\gamma \cdot \boldsymbol{e}_\delta)$. Components $\mu_{3\alpha\beta}$ are translated to the Cartesian basis with the aid of transformation matrix $\boldsymbol{T}$ (C.3) by analogy with (C.2):

$$
\begin{bmatrix} \bar{\mu}_{311} \\ \bar{\mu}_{322} \\ 2\bar{\mu}_{312} \end{bmatrix} = \boldsymbol{T} \begin{bmatrix} \mu_{311} \\ \mu_{322} \\ 2\mu_{312} \end{bmatrix}. \tag{C.11}
$$

Expressions (C.9) and (C.11) hold true also for the components of tensors $\nabla \boldsymbol{\alpha}$ and $\nabla \boldsymbol{\beta}$.

References

[1] G. Maugin, Continuum Mechanics Through the Twentieth Century: A Concise Historical Perspective, Springer Science & Business Media, Dordrecht, 2013.

[2] A. W. McFarland, J. S. Colton, Role of material microstructure in plate stiffness with relevance to microcantilever sensors, Journal of Micromechanics and Microengineering 15 (5) (2005) 1060–1067.

[3] N. A. Fleck, V. S. Deshpande, M. F. Ashby, Micro-architectured materials: past, present and future, Proceedings of the Royal Society A 466 (2010) 2495–2516.

[4] L. R. Meza, A. J. Zelhofer, N. Clarke, A. J. Mateos, D. M. Kochmann, J. R. Greer, Resilient 3d hierarchical architected metamaterials, Proceedings of the National Academy of Sciences 112 (2015) 11502–11507.

[5] E. Barchiesi, M. Spagnuolo, L. Placidi, Mechanical metamaterials: a state of the art, Mathematics and Mechanics of Solidsdoi:https://doi.org/10.1177/1081286517735695.

[6] A. Carcaterra, F. dell'Isola, R. Esposito, M. Pulvirenti, Macroscopic description of microscopically strongly inhomogenous systems: A mathematical basis for the synthesis of higher gradients metamaterials, Archive for Rational Mechanics and Analysis 218 (2015) 1239–1262.

[7] E. Cosserat, F. Cosserat, Théorie des corps déformables, Paris, 1909.

[8] R. D. Mindlin, Micro-structure in linear elasticity, Archive for Rational Mechanics and Analysis 16 (1964) 51–78.

[9] R. D. Mindlin, Second gradient of strain and surface-tension in linear elasticity, International Journal of Solids and Structures 1 (1965) 417–438.

[10] I. Vardoulakis, G. Exadaktylos, E. Aifantis, Gradient elasticity with surface energy: Mode-III crack problem, International Journal of Solids and Structures 33 (1996) 4531–4559.

[11] B. S. Altan, E. C. Aifantis, On some aspects in the special theory of gradient elasticity, Journal of the Mechanical Behavior of Materials 8 (1997) 231–282.

[12] A. Giannakopoulos, K. Stamoulis, Structural analysis of gradient elastic components, International Journal of Solids and Structures 44 (10) (2007) 3440–3451.

[13] C. Liebold, W. H. Müller, Applications of strain gradient theories to the size effect in submicro-structures incl. experimental analysis of elastic material parameters, Bulletin of TICMI 19 (2015) 45–55.

[14] F. dell'Isola, I. Giorgio, M. Pawlikowski, Large deformations of planar extensible beams and pantographic lattices: heuristic homogenization, experimental and numerical examples of equilibrium, Proceedings of the Royal Society of London A 472 (2016) 20150790.

[15] J. Niiranen, V. Balobanov, J. Kiendl, S. Hosseini, Variational formulations, model comparisons and isogeometric analysis for Euler-Bernoulli micro- and nano-beam models of strain gradient elasticity, Mathematics and Mechanics of Solids, https://doi.org/10.1177/1081286517739669.

[16] S. Khakalo, V. Balobanov, J. Niiranen, Modelling size-dependent bending, buckling and vibrations of 2D triangular lattices by strain gradient elasticity models: applications to sandwich beams and auxetics, International Journal of Engineering Science 127 (2018) 33–52.

[17] M. Lazar, G. A. Maugin, E. C. Aifantis, Dislocations in second strain gradient elasticity, International Journal of Solids and Structures 43 (2006) 1787–1817.

[18] S. M. Mousavi, E. C. Aifantis, Dislocation-based gradient elastic fracture mechanics for in-plane analysis of cracks, International Journal of Fracture 202 (1) (2016) 93–110.

[19] H. Askes, E. C. Aifantis, Gradient elasticity in statics and dynamics: An overview of formulations, length scale identification procedures, finite element implementations and new results, International Journal of Solids and Structures 48 (2011) 1962–1990.

[20] J. Altenbach, H. Altenbach, V. A. Eremeyev, On generalized Cosserat-type theories of plates and shells: a short review and bibliography, Archive of Applied Mechanics 80 (2010) 73–92.

[21] K. Lazopoulos, A. Lazopoulos, Nonlinear strain gradient elastic thin shallow shells, European Journal of Mechanics - A/Solids 30 (3) (2011) 286 – 292.

[22] B. Sun, E. C. Aifantis, Gradient elasticity formulations for micro/nanoshells, Journal of Nanomaterials 2014. doi:http://dx.doi.org/10.1155/2014/846370.

[23] S. Papargyri-Beskou, D. Beskos, Stability analysis of gradient elastic circular cylindrical thin shells, International Journal of Engineering Science 47 (11) (2009) 1379–1385.

[24] H. Zeighampour, Y. T. Beni, I. Karimipour, Torsional vibration and static analysis of the cylindrical shell based on strain gradient theory, Arabian Journal for Science and Engineering 41 (5) (2016) 1713–1722.

[25] S. Papargyri-Beskou, S. V. Tsinopoulos, D. E. Beskos, Wave propagation in and free vibrations of gradient elastic circular cylindrical shells, Acta Mechanica 223 (8) (2012) 1789–1807.

[26] S. Thai, H.-T. Thai, T. P. Vo, V. I. Patel, Size-dependant behaviour of functionally graded microplates based on the modified strain gradient elasticity theory and isogeometric analysis, Computers and Structures 190 (2017) 219–241.

[27] J. Niiranen, A. H. Niemi, Variational formulation and general boundary conditions for sixth-order boundary value problems of gradient-elastic Kirchhoff plates, European Journal of Mechanics - A/Solids 61 (2017) 164–179.

[28] J. Niiranen, S. Khakalo, V. Balobanov, A. H. Niemi, Variational formulation and isogeometric analysis for fourth-order boundary value problems of gradient-elastic bar and plane strain/stress problems, Computer Methods in Applied Mechanics and Engineering 308 (2016) 182–211.

[29] S. T. Yaghoubi, V. Balobanov, S. M. Mousavi, J. Niiranen, Variational formulations and isogeometric analysis for the dynamics of anisotropic

gradient-elastic Euler–Bernoulli and shear-deformable beams, European Journal of Mechanics - A/Solids 69 (2018) 113–123.

[30] V. Balobanov, J. Niiranen, Locking-free variational formulations and isogeometric analysis for the Timoshenko beam models of strain gradient and classical elasticity, Computer Methods in Applied Mechanics and Engineering 339 (2018) 137–159.

[31] T. J. R. Hughes, J. A. Cottrell, Y. Bazilevs, Isogeometric analysis: Cad, finite elements, nurbs, exact geometry and mesh refinement, Computer Methods in Applied Mechanics and Engineering 194 (2005) 4135–4195.

[32] F. Cirak, M. Ortiz, P. Schröder, Subdivision surfaces: a new paradigm for thin-shell finite-element analysis, International Journal for Numerical Methods in Engineering 47 (12) (2000) 2039–2072.

[33] J. Kiendl, K.-U. Bletzinger, J. Linhard, R. Wüchner, Isogeometric shell analysis with Kirchhoff–Love elements, Computer Methods in Applied Mechanics and Engineering 198 (49) (2009) 3902–3914.

[34] J. Kiendl, Y. Bazilevs, M.-C. Hsu, R. Wüchner, K.-U. Bletzinger, The bending strip method for isogeometric analysis of Kirchhoff–Love shell structures comprised of multiple patches, Computer Methods in Applied Mechanics and Engineering 199 (37) (2010) 2403–2416.

[35] N. Nguyen-Thanh, N. Valizadeh, M. Nguyen, H. Nguyen-Xuan, X. Zhuang, P. Areias, G. Zi, Y. Bazilevs, L. D. Lorenzis, T. Rabczuk, An extended isogeometric thin shell analysis based on Kirchhoff–Love theory, Computer Methods in Applied Mechanics and Engineering 284 (2015) 265–291.

[36] N. Nguyen-Thanh, K. Zhou, X. Zhuang, P. Areias, H. Nguyen-Xuan, Y. Bazilevs, T. Rabczuk, Isogeometric analysis of large-deformation thin shells using RHT-splines for multiple-patch coupling, Computer Methods in Applied Mechanics and Engineering 316 (2017) 1157–1178.

[37] T. X. Duong, F. Roohbakhshan, R. A. Sauer, A new rotation-free isogeometric thin shell formulation and a corresponding continuity constraint for patch boundaries, Computer Methods in Applied Mechanics and Engineering 316 (2017) 43–83.

[38] S. Khakalo, J. Niiranen, Isogeometric analysis of higher-order gradient elasticity by user elements of a commercial finite element software, Computer-Aided Design 82 (2017) 154–169.

[39] Y. Başar, W. Krätzig, Theory of Shell Structures, 2nd Edition, Fortschritt-Berichte VDI: Reihe 18, Mechanik, Bruchmechanik, VDI-Verlag, 2001.

[40] M. Bischoff, W. Wall, K.-U. Bletzinger, E. Ramm, Models and finite elements for thin-walled structures, in: E. Stein, R. de Borst, T.J.R. Hughes (Eds.), Encyclopedia of Computational Mechanics, Solids, Structures and Coupled Problem (Chapter 3), Vol. 2, John Wiley, 2004.

[41] R. D. Mindlin, N. N. Eshel, On first strain-gradient theories in linear elasticity, International Journal of Solids and Structures 4 (1968) 109–124.

[42] N. Auffray, H. L. Quang, Q. He, Matrix representations for 3D strain-gradient elasticity, Journal of the Mechanics and Physics of Solids 61 (2013) 1202–1223.

[43] M. Lazar, G. Po, The non-singular Green tensor of Mindlin's anisotropic gradient elasticity with separable weak non-locality, Physics Letters A 379 (24-25) (2015) 1538–1543.

[44] M. Lazar, G. A. Maugin, Nonsingular stress and strain fields of dislocations and disclinations in first strain gradient elasticity, International Journal of Engineering Science 43 (2005) 1157–1184.

[45] J. Niiranen, J. Kiendl, A. H. Niemi, A. Reali, Isogeometric analysis for sixth-order boundary value problems of gradient-elastic Kirchhoff plates, Computer Methods in Applied Mechanics and Engineering 316 (2017) 328–348.

[46] D. C. C. Lam, F. Yang, A. C. M. Chong, J. Wang, P. Tong, Experiments and theory in strain gradient elasticity, Journal of the Mechanics and Physics of Solids 51 (2003) 1477–1508.

[47] T. Belytschko, H. Stolarski, W. K. Liu, N. Carpenter, J. Ong, Stress projection for membrane and shear locking in shell finite elements, Computer Methods in Applied Mechanics and Engineering 51 (1) (1985) 221–258.

[48] K.-J. Bathe, A. Iosilevich, D. Chapelle, An evaluation of the MITC shell elements, Computers & Structures 75 (1) (2000) 1–30.

[49] H. Askes, E. C. Aifantis, Gradient elasticity and flexural wave dispersion in carbon nanotubes, Physical Review B 80 (19) (2009) 195412.

[50] J. Niiranen, S. Khakalo, V. Balobanov, Isogeometric finite element analysis of mode i cracks within strain gradient elasticity, Journal of Structural Mechanics 50 (2017) 337–340.